LAMINATED AND HYBRID SOFT ARMOR SYSTEMS FOR BALLISTIC

APPLICATIONS

Except where reference is made to the work of others, the work described in this thesis is my own or was done in collaboration with my advisory committee. This thesis does not include proprietary or classified information.

_____

Hasan Basri Kocer

Certificate of Approval:

_____	_____
Howard L. Thomas, Jr. Associate Professor Polymer & Fiber Engineering	Roy Broughton, Jr., Chair Professor Polymer & Fiber Engineering
_____	_____
Sabit Adanur Professor Polymer & Fiber Engineering	Ann B. Presley Associate Professor Consumer Affairs
_____	_____
Peter Schwartz Professor Polymer & Fiber Engineering	George T. Flowers Interim Dean Graduate School

LAMINATED AND HYBRID SOFT ARMOR SYSTEMS FOR BALLISTIC APPLICATIONS

Hasan Basri Kocer

A Thesis
Submitted to
the Graduate Faculty of
Auburn University
in Partial Fulfillment of the
Requirements for the
Degree of
Master of Science

Auburn, Alabama
December 17, 2007

LAMINATED AND HYBRID SOFT ARMOR SYSTEMS FOR BALLISTIC APPLICATIONS

Hasan Basri Kocer

Permission is granted to Auburn University to make copies of this thesis at its discretion, upon request of individuals or institution and their expense. The author reserves all publication rights.

_____
Signature of Author

_____
Date of Graduation

VITA

Hasan Basri Kocer, son of Mustafa and Nuriye Kocer, was born August 13, 1981 in Bursa, Turkey. He entered Uludag University in September 1999, and graduated a Bachelor of Textile Engineering in July 2003. In spring of 2006, he was enrolled by Auburn University in the Department of Polymer and Fiber Engineering for a Master's degree.

THESIS ABSTRACT

LAMINATED AND HYBRID SOFT ARMOR SYSTEMS FOR BALLISTIC APPLICATIONS

Hasan Basri Kocer

Master of Science, December 17, 2007
(B.S., Uludag University, 2003)

99 Typed Pages

Directed by Roy Broughton, Jr.

The purpose of this study is to investigate the effects of lamination and hybrid soft armor systems through ballistic impact. The investigation was carried out by using tensile, drop-weight impact and actual ballistic testing. The most important conclusions derived from this research are that lamination of the systems with very low resin content are superior to multiple non-laminated systems, and this advance could be improved further by hybrid systems using nonwoven fabric layers on the impact side and relatively tighter woven fabrics between the layers.

ACKNOWLEDGEMENTS

The author would like to express his thanks to his advisor, Dr. Roy Broughton, Jr., for his support, encouragement and valuable advice. The author also expresses his gratitude to the other members of his advisory committee, Dr. Howard Thomas, Dr. Sabit Adanur, Dr. Peter Schwartz and Dr. Ann B. Presley, for their constructive criticism and advice. Thanks to the Department of Polymer and Fiber Engineering for providing support and welcoming environment.

He would like to express his most sincere thanks to his parents, his two sisters, and his brother, whom he treasures mostly, for providing ongoing encouragement and support throughout the years. He would also like to express his appreciation to God for providing him his skills and the ability to think.

Style manual or journal used: The Harvard Journal style

Computer software used: Microsoft Office Word 2002, Microsoft Excel 2002

TABLE OF CONTENTS

LIST OF FIGURES xi

LIST OF TABLES xiv

CHAPTER ONE: INTRODUCTION 1

CHAPTER TWO: LITERATURE REVIEW 3

2.1 The History of Ballistic Protection 3

2.2 Soft Body Armor Protection Systems 4

2.3 Importance and Usage of Textile Materials in Soft Body Armor 5

2.4 Importance of Nonwoven and Low Resin Compliant Laminate Usage in Ballistic Textile Materials 7

2.5 Hybrid Armor Systems 8

2.6 Impact Behavior of the Linear Elastic Materials 9

2.6.1 Transverse Impact Behavior of a Single Yarn 9

2.6.2 Transverse Impact of a Single Ply of Fabric 11

2.7 Mechanisms Influencing the Ballistic Performance of the Systems 13

2.7.1 Material Properties 13

2.7.2 Fabric Structure 14

2.7.3 Projectile Geometry 16

2.7.4 Impact Velocity 17

2.7.5 Friction and Lamination 18

2.7.6 Test Conditions 19
2.8 Fabric Deformation under Ballistic Impact 20
2.9 Ballistic Impact Energy Absorption Mechanisms by Multi-Ply Fabric System 22
2.9.1 Pyramid Formation on the Back Face of the Target 23
2.9.2 Energy Absorption by Deformation of the Primary Yarns 24
2.9.3 Energy Absorption by Deformation of the Secondary Yarns 25
2.9.4 Energy Absorption due to Delamination 26
2.9.5 Energy Absorption by Friction Mechanism 27
2.9.6 Energy Absorption Mechanism of Nonwoven Structures 28
2.10 The Amount of the Absorbed Energy in a Ballistic Impact Event 29
2.11 Equipment Standards for Ballistic Resistance of Personal Body Armor 31
2.11.1 Baseline Ballistic Limit 33
2.11.2 Penetration 33
2.11.3 Backface Signature (BFS) 33
CHAPTER THREE: METHODOLOGY 34
3.1 Composition of the Materials 34
3.2 Sample Preparation for Shear and Peel Tests 35
3.3 Sample Preparation for Drop-Weight Impact and Ballistic Tests 36
3.4 Experimental Setups 37
CHAPTER FOUR: RESULTS AND DISCUSSION 42
4.1 Shear and Peel Test Results 42
4.2 Drop-Weight Impact Test Results 45
4.3 Ballistic Test Results 52

4.4 Postmortem Inspection 63
CHAPTER FIVE: CONCLUSIONS 70
REFERENCES 72
APPENDICES 76
Appendix A. Fiber Mechanical Properties 76
Appendix B. Experimental Setup for Ballistic Test 77
Appendix C. Cohesive Failure of Laminated Fabrics 78
Appendix D. Relative Energy Absorption of Three Different Type of Bullets Through 1, 2 and 3 Layers of BG Fabric 79
Appendix E. Drop-Weight Impact Test Results of EAA Polymer Film 79
Appendix F. Cunniff Ballistic Limit Approach 80
Appendix G. Naik-Shrirao-Reddy Ballistic Limit Approach 81
Appendix H. Landa-Olivares Ballistic Limit Approach 84
Appendix I. Chemical Structures of the Polymer Films 85

LIST OF FIGURES

Figure 1. Transverse Impact on a Single Yarn 10

Figure 2. Transverse Impact on a Single Ply of Fabric..... 12

Figure 3. The “Wedge Through” Phenomenon 15

Figure 4. Projectiles with Different Geometries..... 16

Figure 5. Cutting Action with Flat Nose Projectiles..... 17

Figure 6. Different Yarn Deformation Mechanisms Due to Boundary Conditions..... 20

Figure 7. Fabric Deformation under Ballistic Impact..... 21

Figure 8. Representation of the Energy Absorption due to Pyramid Formation 24

Figure 9. Shape of Delamination Region..... 27

Figure 10. Fabric Energy Absorption due to Variable Impact Velocities 31

Figure 11. Representation of Sample Preparation and Testing for Peel Tests..... 36

Figure 12. Representation of Sample Preparation and Testing for Shear Tests 36

Figure 13. Standard (a) and Modified (b) Tip of the Drop-Weight Impact Tester..... 38

Figure 14. Top View of the Lower Clamp..... 39

Figure 15. Bullets Used in Ballistic Tests..... 40

Figure 16. Experimental Setup for Ballistic Tests..... 41

Figure 17. Results of Shear Test..... 42

Figure 18. Shear Behavior of the Polymer Films 43

Figure 19. Result of Peel Tests..... 44

Figure 20. Energy Absorption of Single and Multi Layer BG Fabrics 47
Figure 21. Energy Absorption of Single and Multi Layer KPG Fabrics 48
Figure 22. Energy Absorption of Laminated BG Fabrics 49
Figure 23. Energy Absorption of Laminated BG Fabrics Hybridized with Outer Nonwoven Layer 49
Figure 24. Energy Absorption of Nonwoven Facing 50
Figure 25. Nonwoven Layer Movement through Inner Layers 50
Figure 26. Comparison of Fabric-Fabric Lamination vs. Fabric-Nonwoven Lamination 51
Figure 27. Sand Scattering between BG Fabrics 53
Figure 28. Ballistic Behavior of the BG Fabrics 55
Figure 29. Ballistic Test Results of Laminated Structures 56
Figure 30. Ballistic Test Results of Laminated Structures II(0.22 Short HV) 56
Figure 31. Ballistic Test Results of Laminated Structures III (0.22 Magnum Flat Nose).57
Figure 32. Ballistic Test Results of Nonwoven Facing Usage I 57
Figure 33. Ballistic Test Results of Nonwoven Facing Usage II (0.22 Short HV) 58
Figure 34. Ballistic Test Results of the Nonwoven Facing Usage III (0.22 Magnum Flat Nose) 59
Figure 35. Ballistic Test Results for Compositions Containing KPG Fabrics I 59
Figure 36. Ballistic Test Results for Compositions Containing KPG Fabrics II (0.22 Short HV) 60
Figure 37. Ballistic Test Results for Compositions Containing KPG Fabrics III (0.22 Magnum Flat Nose) 61

Figure 38. Ballistic Test Results of the Composite and Sand Scattered Structures I (0.22 Short HV)..... 62
Figure 39. Ballistic Test Results of the Composite and Sand Scattered Structures II (0.22 Magnum Flat Nose) 62
Figure 40. Pyramid Formation on the Back Face of the Target..... 64
Figure 41. Back Face Deformation of the Targets in the Ballistic Tests with Sharp Nose Magnum Bullets a) 1 BG +1NW b) 2BG + 1NW 64
Figure 42. Transit of Nonwoven Layer through the Target I (target: 1BG+1NW, bullet: 0.22 Short)..... 65
Figure 43. Transit of Nonwoven Layer through the Target II (target: 1BG+1NW, bullet: 0.22 Short)..... 65
Figure 44. Transit of Nonwoven Layer through the Target III (target: 2BG+1NW, bullet: 0.22 Short)..... 66
Figure 45. Laterally Restricted Primary Yarns (target: 2BG+1NW, bullet: 0.22 Short).. 66
Figure 46. Bullet Mark on the Front Face of the Target after Reflection (target: 2BG-Laminated, bullet: 0.22 Short) 67
Figure 47. Backface Deformation of the Target through Reflection (Target: 2BG-Laminated, Bullet: 0.22 Short)..... 67
Figure 48. Delamination between the BG Fabrics in the Impact Zone 68
Figure 49. Shape Deformation on the Bullets I (a) original (b) deformed 68
Figure 50. Shape Deformation on the Bullets II (a) original (b,c,d) deformed 69

LIST OF TABLES

Table 1. NIJ Standard 0101.04 Classification 32

Table 2. Specifications of Adhesive Polymers 35

Table 3. Bullet Specifications Used in Ballistic Tests 40

Table 4. Composition of the Samples for Drop-Weight Impact Test 45

Table 5. Drop-Weight Impact Test Results 46

Table 6. Composition of the Samples for the Ballistic Test 52

Table 7. Ballistic Test Results 54

CHAPTER ONE: INTRODUCTION

Textile-based soft body armor offers significant contributions to ballistic protection for military and law enforcement personnel by their lightweight structures. The present systems, constructed from conventional textile materials including woven fabrics and laid-up filament composites, have become relatively thicker and heavier to meet increasing protection requirements against more effective threats. Hence, it is desirable to construct ballistic protective systems providing higher protection without sacrificing mobility and comfort.

To construct ballistic protective systems successfully, it is important to have an understanding of the behavior of the structures during ballistic impact event. Researchers state a clear indication that yarn straining and finally breaking is the primary mechanism of the total energy absorption. The most significant circumstances that cause systems to show worse performance are the sliding of pointed nose bullets between the yarns and the cutting ability of sharp edged bullets. The sliding-through action results in less yarn straining while the cutting action results in early breakage of the yarns.

In recent years, ballistic-grade composites have been used to reduce the sliding-through action of the bullet by their more stable structures that restrict the lateral movement of the yarns during the ballistic impact event. The presence of a small amount of resin (20%) increases the energy absorption while higher resin contents produce worse performance because highly restricted yarns do not share the load effectively.

Nonwoven fabrics are being used in ballistic protection applications because of their mechanically unique and lightweight structures. Less fiber failure occurs in the nonwoven structures under the ballistic impact compared to woven and unidirectional structures. They offer significant resistance to the cutting action of sharp edge nose bullets when used as a facing on the systems.

The purpose of this study is to investigate the effects of lamination and hybrid soft armor systems during ballistic impact. The goals of the study are to keep as many yarns as possible in front of the bullet and to prevent yarns shearing from the impact of sharp edge bullets during the ballistic impact event. It was thought that using adhesive polymer films between the layers would restrict the lateral movement of yarns, and that nonwoven structures used as a facing on the systems might reduce the cutting effect of the bullets. Lightweight hybrid armor systems might, therefore, offer higher energy absorption against different threats.

CHAPTER TWO: LITERATURE REVIEW

This chapter starts with description of the ballistic protection and the importance of textile materials in soft body armor, followed by a discussion of the material behavior during the ballistic impact event. Lastly, the chapter describes the mechanisms influencing the ballistic performance of the systems.

2.1 The History of Ballistic Protection

Mankind has used textiles and ductile laminates for bodily protection since ancient times. The development of armor has always run parallel to the development of increasingly efficient weaponry on the battlefield throughout human history [1]. The arms race between civilizations forced them to create better protection without sacrificing personal mobility.

One of the earliest forms of soft body armor was animal skins. These offered more protection than other forms of armor with the advantage of being lightweight. In the 8th century, chain mail was introduced; a shirt of interlocked metal rings, weighing around 14-30 lbs. It was used for hundreds of years in different forms. Probably the heaviest body armor throughout the history is the medieval suit of armor. From about 1200 to the 1600s, medieval knights seeking greater protection covered themselves in whole suits constructed of metal plate armor. While this armor was quite effective for the threats of the time, it was extremely heavy weighing about 60 lbs. The advance of gunpowder firearms caused its disappearance [2].

In contrast to the suits of armor, the medieval Japanese used silk for protection. This produced the oldest bullet resistant fabric vest [3]. It was even considered for use as ballistic protection in the United States as late as the early 1900s. This natural fabric was strong, lightweight and provided effective protection against low velocity weapons but was not able to stop new higher velocity firearms.

The advance of firearms made all of these forms of protection obsolete until the development of high strength, and high modulus fibers in the 1960s [6]. During World War II, the next step toward the softer body armor was when the military began using the "flak jacket" which was constructed of ballistic polyamides. The flak jackets helped shield personnel against munitions fragment but could not protect against most rifles and pistols [2]. The current state-of-the-art body armor system being fielded by the US Army is the Interceptor, consisting of an outer tactical vest made of Kevlar® KM2 weave that is able to stop high-powered handgun ammunition. The interceptor body armor system weighs 16.4 lbs. where the previous body armor, the flak jacket, weighed 25.1 lbs [5].

2.2 Soft Body Armor Protection Systems

Modern body armor systems are divided into two main categories as hard body armor and soft body armor systems. The hard body armor system, made of thick ceramic or metal plates, functions similar to as the iron suits worn by medieval knights. It is hard enough to deflect a bullet and prevents penetration. Typically, hard body armor offers more protection than soft body armor, but it is much heavier and reduces its wearer's mobility and comfort. Police officers and military personnel may wear this sort of protection when there is a high risk of attack. For daily use, they generally prefer to wear

soft body armor which offers flexible protection although it is stiffer and heavier than an ordinary shirt or jacket [4].

Generally, a soft body armor system is constructed by multiple layers of ballistic fabrics and a carrier made of conventional garment fabric. Its functionality differs from hard body armor; soft body armor gradually slows the projectile and finally catches it during a ballistic impact event. The impact energy is absorbed by different energy absorbing mechanisms. The impact resistance of a soft armor depends on its capability to absorb energy locally at the impact zone and disperse energy rapidly out of the impact zone. These characteristics are determined by a number of factors; fiber intrinsic physical properties, fabric structure characteristics, number of fabric layers, projectile shape, mass and material properties, impact velocity, and interfacial friction characteristics within impact system [7].

Lightweight soft armor is used in situations where heavier hard armor cannot be used because of weight and comfort limitations. Major applications fields are: personal protection, armoring of vehicles, helicopters, patrol boats and transportable shelters.

2.3 Importance and Usage of Textile Materials in Soft Body Armor

The development of lightweight fibrous material systems providing protection from high velocity bullets has been an important research topic since World War II and is getting more important with new developments in the weaponry industry. The most effective soft body armor for military and law enforcement personnel are constructed by multi-ply fabrics and flexible fibrous composites. These fibrous materials are also used in armor panels for automobiles and light military vehicles [8].

Fibrous material systems for ballistic protection were significantly improved in the last few decades. Nylon fibers were leading the industry prior to 1970s.These fibers showed considerable non-linearity in stress-strain behavior, with relatively high strain values to failure. In the last few decades, new high performance fibers have been developed that exhibit greatly improved physical performance. These polymers include aramids (e.g., Kevlar®, Twaron®, Technora®), highly oriented polyethylene (e.g., Spectra®, Dyneema®) and PBO (e.g., Zylon®). All these materials show more advanced physical characteristics from their nylon predecessors by having; relatively very high stiffness (although sufficiently flexible), extremely high strength to weight ratios, and very low strains to failure (<4%). Since, weight and flexibility are two of the most important design parameters for soft body armor, those polymers have been widely used in making soft body armor since their introduction to market [8]. They are essentially elastic in tension, both at low and high rates of loadings and at the same time they are similar to nylon in transverse compression, undergoing large plastic deformation without a significant reduction in tensile load carrying ability [8].

The aramids are the most common fibers used in the production soft body armor. Aramid fibers, Kevlar 129®, KM2, Twaron etc., consist of highly aligned macromolecules resulting in excellent tenacity and modulus; thus, making them ideal for ballistic protection applications. The lightness of these materials increases their popularity.

2.4 Importance of Nonwoven and Low Resin Compliant Laminate Usage in Ballistic Textile Materials

Today, nonwoven materials are being used in ballistic protection applications because of their light weight and flexibility. The use of nonwoven fabrics in the market began in the late 1960s. In a study by the U.S. Department of Defense, a needle-punched nonwoven structure containing nylon fibers was produced at one-third the weight of a woven fabric, while retaining 80% of its ballistic resistance [11]. In another study by Thomas [12], it has been shown that a blend of para-aramid and high density polyethylene (50/50) needle-punched nonwoven fabric proves a better ballistic performance than a 100% para-aramid plain woven structure.

The usual method to increase the protection against more lethal ballistic threats is to add more layers of fabric or ceramic inserts with drawbacks of increased weight of the armor and reduced mobility of the user. In recent years, textile composites are being used in ballistic protection applications because of their higher energy absorption characteristics and lightweight properties. Woven fabrics are impregnated with resin to form a unique class of structural composites, so called “ballistic-grade” or “armor-grade” composites. The armor-grade composites are constructed with very low resin content, around 20% by volume, to achieve maximum utilization of intrinsically high resistance fibers to the transverse impact. As a result of very low resin content, these composites are relatively flexible unless a structure of considerable thickness is constructed.

2.5 Hybrid Armor Systems

Prosser et al. [13] found that the layer close to the impact surface behaves inelastically, whereas the layers toward the back behave elastically when multi ply armor systems are impacted by sharp-edged projectiles. Cunniff [14] has also studied this decoupled response through the thickness of multi-ply systems and notes that the armor system response is dominated by the inelastic behavior of the material when impacted with sufficiently high velocities. He has investigated hybrid armor systems by replacing the material at the impact face with a different material and proved that the ballistic performance of the armor system can still be maintained while improving the other properties such as lightness of the system.

Such hybrid systems have also been investigated by Thomas [12]. He found that using a nonwoven facing on a woven fabric provided enhanced protection against handgun threats rather than just Spectra Shield ® alone. Further improvement was found by using a Spectra Shield ® facing on the nonwoven facing.

Hybridization of the armor, through its thickness, has been used for ballistic protection applications recently and can be seen by the number of patents as well as commercially available soft armor systems consisting of multiple materials. However, few reports exist in the open literature detailing the effect of the hybridization on ballistic performance. It appears that studies are ongoing to optimize the performance of ballistic textiles through hybrid fabrics and compliant composite laminate systems by layering of different materials and even different textiles.

2.6 Impact Behavior of the Linear Elastic Materials

First of all, the impact behavior of the ballistic material should be understood clearly, in order to optimize the design of soft body armor or to increase its ballistic resistance while keeping or even reducing its weight and rigidity. The best way to understand the impact behavior of armor systems is to study the impact behavior of structure's construction units such as single layer fabric and single yarn.

Numerous experimental and theoretical works have been conducted to understand the transverse impact behavior of single yarns and single layer fabrics, during the past several decades. Smith et al. [15], Roylance [16], and Morrison [17] studied the response of yarns to high speed transverse impact while Wilde et al. [18], Briscoe and Motamedi [19], and Shim et al. [20] investigated the response of single layer fabrics.

2.6.1 Transverse Impact Behavior of a Single Yarn

An investigation on the transverse impact behavior of a single yarn might be the best starting point for further advance on the transverse behavior of the fabrics. High velocity ballistic impact causes the local target materials behave like fluids and result in wave propagation in the structure. When a single yarn is struck transversely; two waves, longitudinal and transverse, propagate from the point of impact as shown in Figure 1. The longitudinal tensile wave travels through the fiber axis at the speed of sound in material. During the longitudinal wave propagation, the material behind the longitudinal wave front flows toward the impact point, which has deflected in the direction of motion of the impacting projectile. This transverse movement of the fiber is the transverse wave, which propagates at a velocity lower than the longitudinal wave [6].

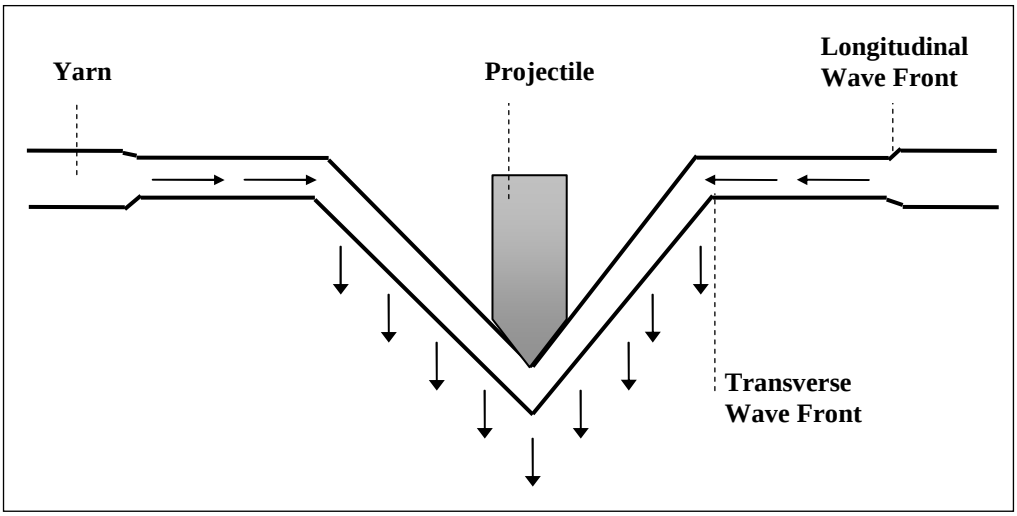

Figure 1. Transverse Impact on a Single Yarn

Figure 1 shows a projectile transversely impacting on a long straight yarn. The longitudinal wave speed, c (m/s), is given by (Smith et al. [21]);

$$c = \sqrt{\frac{E}{\rho}}$$

where the yarn tensile elastic modulus is E (Pa), and volumetric density is ρ (kg/m^3).

The strain on the yarn is zero ahead of the longitudinal wave front, and a constant tensile strain is developed behind of the wave front. The tensile strain "ε" is determined by the yarn tensile elastic modulus E, volumetric density ρ, and the impact velocity υ. It is given by;

$$2\varepsilon\sqrt{\varepsilon(1+\varepsilon)} - \varepsilon^2 = \frac{\rho\upsilon^2}{E}$$

The transverse wave propagates away from the impact point at a relatively lower speed and its wave speed, u (m/s), is given by;

$$u = c\sqrt{\frac{\varepsilon}{1+\varepsilon}}$$

The strain of the yarn does not change ahead of the transverse wave front but the motion of the yarn shows a rapid change. Ahead of the transverse wave front but behind the longitudinal wave front, yarn moves longitudinally toward the impact point. Behind the transverse wave front, yarn material moves transversely in the impact direction.

2.6.2 Transverse Impact of a Single Ply of Fabric

The response of the transverse impact of a single ply of fabric shows similarities with a single fiber. Cunniff [22] notes that when a projectile impacts the fabric, analogous transverse and longitudinal waves develop and propagate away from the impact point in the principal yarns that are direct contact with the projectile. Additionally, orthogonal yarns defined as yarns that intersect the principal yarns, are then pulled out of the original fabric plane by the transverse deflection of the principal yarns. These orthogonal yarns undergo a deformation and develop waves like those observed in the principal yarns.

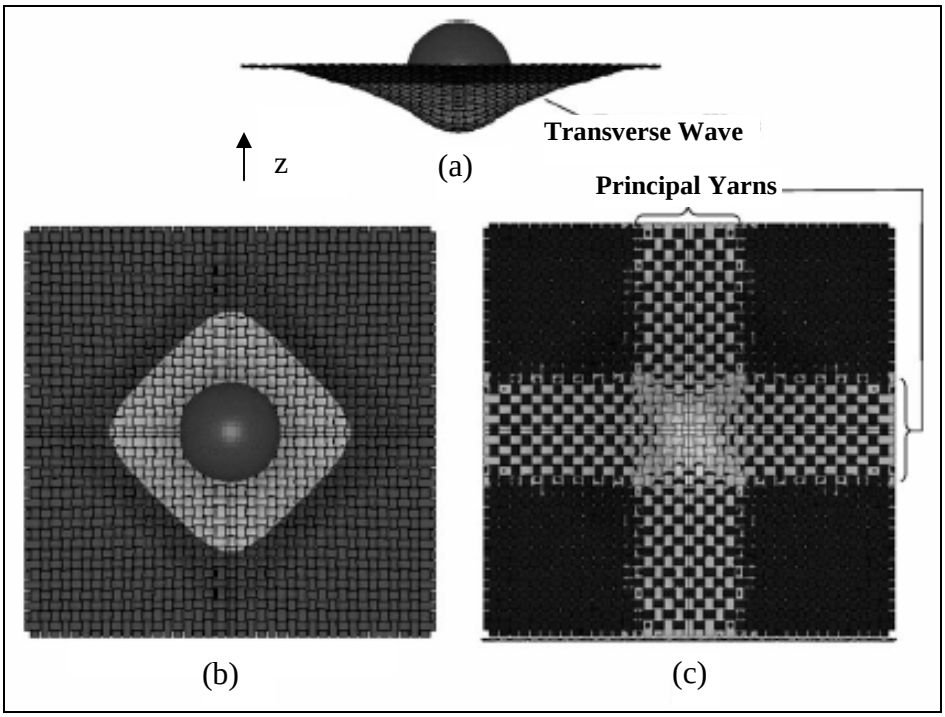

Figure 2. Transverse Impact on a Single Ply of Fabric (a) side view, (b) top view of z displacement contours and (c) bottom view showing principal yarns under high stress [6]

Roylance [23] has observed that the wave velocity in a fabric c` is a fixed fraction of the wave velocity in a single fiber c;

$$c` = \frac{c}{\alpha}$$

According to Roylance, α might be attributed to the effective increase of linear density caused by crossovers. He explains that the linear density of a fiber along which the longitudinal wave is propagating is effectively doubled in a square woven fabric. This retards the wave velocity according to the expression for wave speed c by a factor of $\alpha = (2)^{1/2}$.

2.7 Mechanisms Influencing the Ballistic Performance of the Systems

In order to achieve optimal impact protection capabilities, the dynamic mechanical response of the system should be clearly understood. This is often complicated by multiple stress wave interactions at yarn crossovers and making the problem almost analytically intractable. But an investigation on the mechanisms influencing into the mechanical response could make the solution more accessible. Ballistic performance of the systems is affected by a number of mechanisms which include material characteristics, structural construction and properties, projectile characteristics and impact conditions. All of the mechanisms are described individually in the following sections but it should be noted that the mechanisms have been reported in interrelated manner because of the difficulty to isolate them separately.

2.7.1 Material Properties

Roylance and Wang [23] have shown that materials possessing a high modulus and low density (higher longitudinal wave velocity) disperse the strain wave rapidly away from the impact point, which distributes the energy over a wider area and prevents large strains from developing at the impact point. Field and Sun [24] showed that materials having higher wave velocities were advantageous since the stress and strains could propagate more quickly to neighboring fibers and layers, thus involving more material in the ballistic event.

Although ultimate tensile strength and strain of a yarn play a large role in ballistic performance, each of them does not control it alone. Prosser et al. [13] noted that nylon would show higher ballistic performance than Kevlar® if the ballistic performance were based solely on yarn toughness. Recently, Cunniff [25] assumed that fiber specific

toughness and fiber longitudinal wave velocity are the only essential mechanical properties of the system and he has derived a dimensionless fiber property U^* defined as the product of the yarn specific toughness multiplied by its strain wave velocity.

$$U^* = (\frac{\sigma\varepsilon}{2\rho}\sqrt{\frac{E}{\rho}})^{1/3}$$

where σ is the fiber ultimate strength, ε is the fiber ultimate tensile strain. Cunniff developed this property U^* as a first level screening tool to evaluate the performance of fibers, and he noted that the mechanical performance of the systems could be correlated to the mechanical performance of the fibers but could not be determined.

2.7.2 Fabric Structure

The response of a bullet resistant system could be determined from the material properties and the fabric geometry which combine to produce a structural response. It has been observed that loosely woven fabrics and fabrics with unbalanced weaves result in inferior ballistic performance [22].

Weave patterns typically used for ballistic applications are plain and basket weaves. Many studies have analyzed the deformation of a plain weave when subjected to a transverse impact. But the effect of weaving on yarns under transverse impact is not well understood yet.

Chitrangad [26] noted that fabrics should have cover factors, defined as density of the weave, from 0.6 to 0.95 to be effective when utilized in ballistic applications. Yarns are typically damaged by the weaving process when cover factors are greater than 0.95, and the fabrics may be too loose for a proper response when cover factors fall

below 0.6. Loosely woven fabrics might show a worse performance by having the projectile slide-through action instead of wedge through between the yarn mesh.

The wedge through phenomenon, has been studied by several researchers, and is described as the hole formed in the perforated fabric which is smaller in diameter than the projectile and that the number of broken yarns is less than the number of yarns that intersect the projectile [6]. Therefore, lateral movement of the yarns results in less energy absorption.

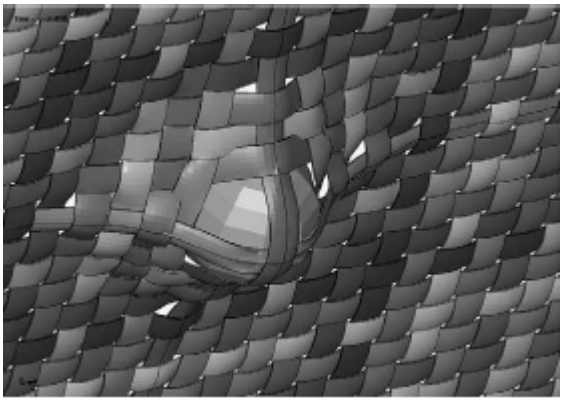

Figure 3. The "Wedge Through" Phenomenon [6]

The lateral movement of the principal yarns can be reduced by increasing the tightness of the fabrics. However, another fabric structural property, crimp, influences the ballistic performance. Crimp is the undulation of the yarns resulting from interweaving. The yarns of a more crimped structure need more time to decrimp during the ballistic impact event (~100μs) and as a result are broken before sufficient elongations to reach maximum energy absorption. Chitrangad [26] has proposed that the weft yarns have larger elongation to break because of their less crimped structure. They would break before the warp yarns and result in less number of broken warp yarns.

The primary yarn mobility can be minimized by using a matrix that allows structural designs for higher energy absorption without sacrificing the higher yarn elongation experienced in highly crimped structures.

2.7.3 Projectile Geometry

The predominant mechanisms that lead to perforation of the fabric are highly dependent on the shape of the projectile and vary with different projectile shapes.

Figure 4 shows the common types of different projectile tip shapes. Among the four shapes, the conical and ogival projectiles perforate the fabric with the least amount of energy absorption because of their ability to slip through the weave. The aerodynamic profiles of their nose shapes enable them to slip through between the yarns while reducing the yarns strain and the number of broken yarns.

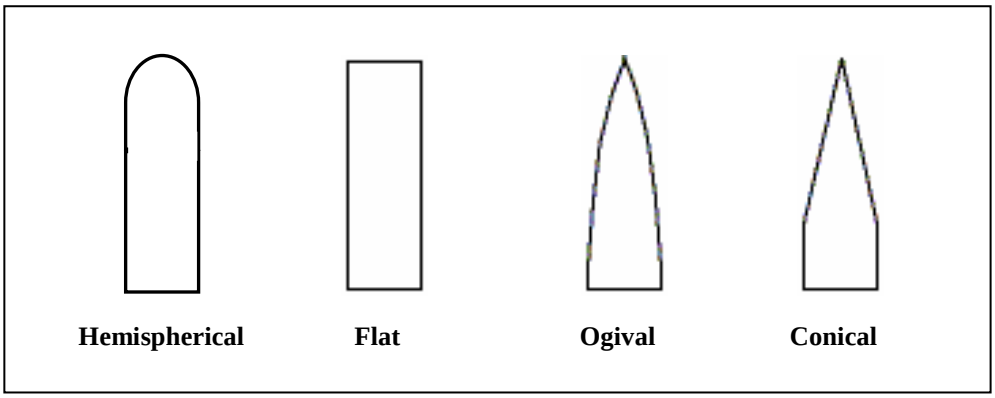

Figure 4. Projectiles with Different Geometries

On the other hand, flat head projectiles have sharp edge which has potential to shear the yarns. The energy absorption through such cutting action is much less than stretching a yarn to breakage [27]. As shown in Figure 5, the first few layers of the multiple layer systems were punched out in the shape of the leading surface of the projectile. Tan et al. [27] have noted that the reinforcement factor for two plies of fabric

is not observed for flat headed projectiles, due to the cutting action of their sharp edges. They also reported that effect of bullet geometry decreases as the number of plies increases.

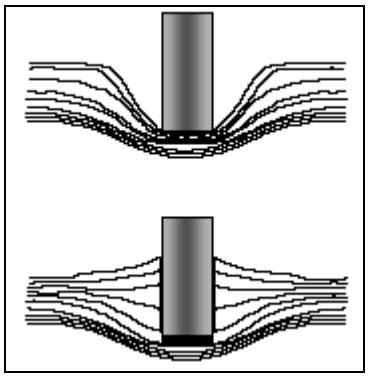

Figure 5. Cutting Action with Flat Nose Projectiles

The hemispherical projectiles are the easiest to stop in the ballistic impact. It is more difficult for the hemispherical projectile to slip through the fabric and the perforation is facilitated mainly by breaking of the primary yarns by straining which leads to more energy absorption.

2.7.4 Impact Velocity

The impact velocity of a projectile highly influences the performance of the protective systems. Low impact velocities below the critical velocity (V_{50}), the velocity at which 50% of the projectiles perforate the target, allow the fabric to absorb more energy because the yarns do not fail during the initial stress rise and the transverse deflection of the fabric has time to propagate. High impact velocities greater than V_{50} cause the damage to localize and the yarns to fail before significant transverse deflection can develop [20]. Cunniff reported that at the impact velocities, much higher than the ballistic limit of a textile armor system, material near the impact surface fails before significant

strain energy is absorbed. He also reported that in this velocity regime, the bulk of the energy absorbed depends primarily on the areal density of the target and the amount of material involved. He termed such impact as an inelastic impact [14].

2.7.5 Friction and Lamination

Friction affects the impact performance of the textile based systems both directly and indirectly. The friction between the yarns and the projectile is considered as the direct effect while the friction between the yarns themselves as the indirect effect.

Chitrangad and Parada [40] showed that the use of finishes on aramid yarns provides higher fiber-fiber friction coefficients and improves ballistic properties of the textile based materials. But they noted that the finishes should be applied onto the fabrics which are ready to use, to avoid from damages in processing. Lee et al. [28] has investigated restricting lateral mobility of yarns by using small amount of resin to increase the number of yarns contacted with projectile during the impact event and to increase the number of broken yarns that results in higher energy absorption. They found that the resin itself did not absorb significant amounts of energy but it certainly had an indirect effect on the energy absorption capacity of the system by influencing the number of yarns broken.

The ballistic impact into multiple ply compliant laminates has been investigated primarily through by experimental designs. The ballistic performance of the materials is generally evaluated in the form of the residual velocity of a projectile and its striking velocity. Damage mechanisms according to delamination are dependent on the properties of the resin and fibers and the fiber-resin adhesion. It is noted that weak fiber-resin adhesion results in complete delamination and is more adequate for the ballistic

applications. Complete delamination of the compliant laminate allows the fibers to extend higher failure strains and does not reduce the wave velocities [6].

2.7.6 Test Conditions

Test conditions, such as the size of the specimen and clamping of the specimen onto edges, significantly affect the stress distribution pattern in the fabrics. Cunniff [22] tested multiple plies of fabrics and observed that the ballistic limit of the fabric was reduced strongly with the smaller departures that restrict the amount of the transverse and longitudinal deflection. However, the size of the target is insignificant above the ballistic limits because of the perforation without significant transverse deflection.

Clamped or unclamped boundary conditions of the material have a significant influence on the material impact behavior during the impact tests. Figure 6, shows the different yarn deformation mechanisms when both of its ends are clamped and when they are free. The yarn is broken at the impact point when its two ends are clamped and not broken when its two ends are left free. In the first situation, when the longitudinal wave reaches the clamped ends, it is reflected back and propagates toward the impact point and cause the tensile stress to be doubled to reach the failure criterion. In the second situation, when the longitudinal wave reaches the free ends, it is also reflected back and propagates toward the impact point but behind the reflected wave front, the yarn tensile stress becomes zero. The fabric boundary condition does not matter when the impact velocity is high enough to break yarns instantaneously while the fabric deformation is localized at the impact region [7].

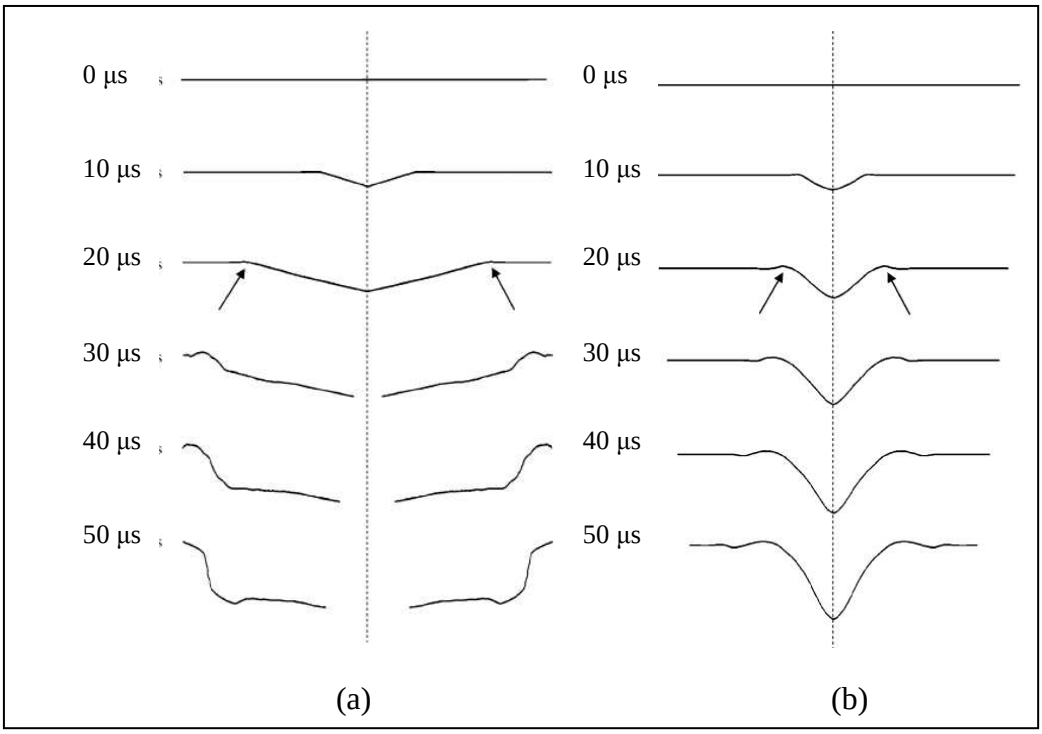

Figure 6. Different Yarn Deformation Mechanisms Due to Boundary Conditions (a) Clamped (b) Unclamped [7]

Insufficient clamping pressure is another important issue that might cause inconsistent results. Slippage on the clamps causes higher energy absorption than the non-slippage cases. But when the clamping force exceeds the level which is not allowing any sliding, energy absorption becomes independent from the clamping force.

2.8 Fabric Deformation under Ballistic Impact

After the initial momentum transfer, local fabric in the impact zone moves together with the projectile. For a balanced ballistic grade woven fabric, the deformation during the impact event occurs in the shape of a pyramid with a rhombus shaped bottom region, in which the diagonal line length of the rhombus bottom is the length of the primary yarn in transverse wave region.

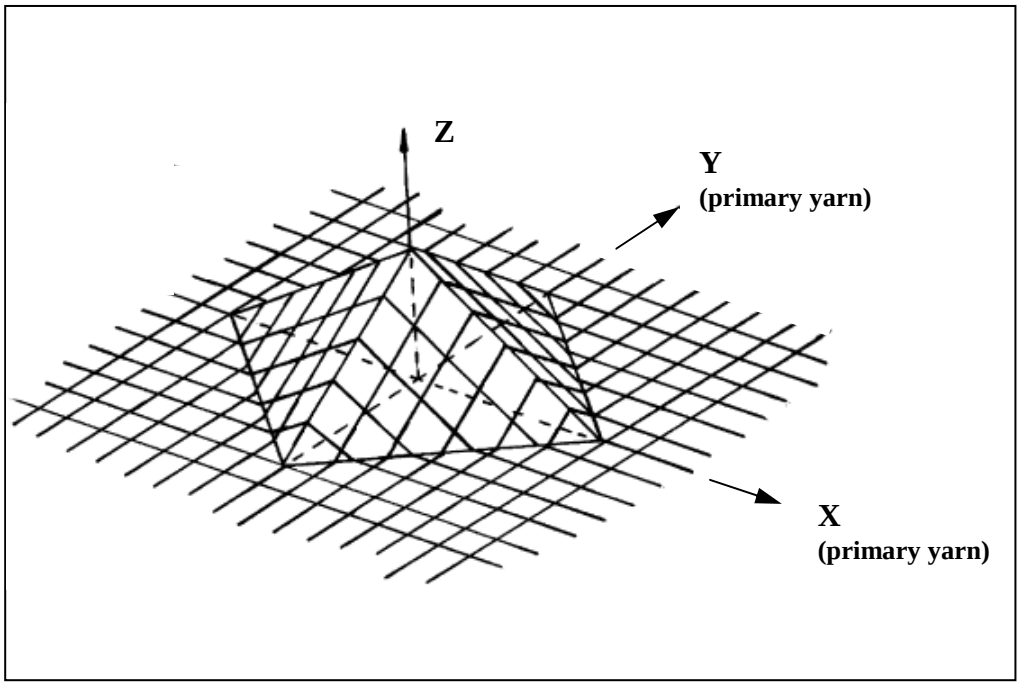

Figure 7. Fabric Deformation under Ballistic Impact

Leech et al. [29] showed that, for a plain woven fabric, the transverse wave front is a rhombus with sides given by the following equation;

$$t = \pm\frac{x}{u_x} \pm \frac{y}{u_y}$$

where x and y are the spatial coordinates of the front at time t, and u_x and u_y are the velocity of transverse waves in the x and y directions, respectively. For plain woven fabric in which the properties of warp yarns equals to that of weft yarns, it can be deduced that $u_x = u_y$ [30].

The ballistic impact event could be ended in three different states. In the first case, the projectile perforates the target and exits with certain velocity, indicating the projectile initial energy was more than the energy that target can absorb. In the second case, the projectile partially penetrates the target, indicating that the projectile initial energy was less than the energy that the target can absorb. Eventually, the projectile can

either be stuck within the target or rebounded. In the third case, the projectile perforates the target completely with zero exit velocity while the initial velocity of the projectile is termed as ballistic limit.

2.9 Ballistic Impact Energy Absorption Mechanisms by Multi-Ply Fabric Systems

Kinetic energy of the projectile is dissipated and absorbed in various ways by the target during a ballistic impact event. The main energy absorbing mechanisms during ballistic impact are: kinetic energy absorbed by the moving pyramid formed on the back face of the target (E_{KE}), energy absorbed due to tensile failure of the primary yarns (E_{TF}), energy absorbed due to elastic deformation of the secondary yarns (E_{ED}), energy absorbed due to delamination (E_{DL}) and frictional energy absorbed during penetration (E_F). The total kinetic energy of the projectile that is lost during ballistic impact is the total energy that is absorbed by the target and could be given by [31];

$$E_{TOTAL} = E_{KE} + E_{TF} + E_{ED} + E_{DL} + E_F$$

The projectile is decelerated very quickly at initial stage of the impact. At this moment the projectile momentum is transferred to the local fabric while the fabric located out of the impact zone is not affected at all. The initial momentum transfer is responsible for the abrupt drop of the projectile velocity at the initial stage. After the initial stage, pyramid formation starts to develop on the back face of the target. As time progresses, the mass of the pyramid increases while its velocity decreases. The yarns are strained and absorb some energy while the pyramid formation takes place. Secondary yarns absorb some energy because of the tension in the yarns. The primary yarns, which afford the resistive force to the projectile motion, are strained the most which leads to

their failure. Tensile failure of the yarns thus absorbs some energy of the projectile. During the ballistic impact event, delamination takes place in the laminated area [31].

2.9.1 Pyramid Formation on the Back Face of the Target

The pyramid formation on the back face of the target can be explained on the basis of transverse wave propagation. During the impact event, the velocity of the moving pyramid is equal to the velocity of the projectile, and the distance traveled by the projectile and the depth of the pyramid formed is equal. The mass of the pyramid increases in descending trend while its velocity decreases.

As shown in Figure 8, higher strain occurs on the primary yarns, correlated to their location with respect to the tip of the projectile. Additionally, the outer layers (closer to impact side) of the laminated system get compressed when the pyramid is being formed, causes higher strain values in the outer layers than the inner layers. The amount of the compression in the outer layers is based on the stress at the point of impact which causes an extra straining of the outer layers. The variation of strain through the thickness direction is assumed to be linear.

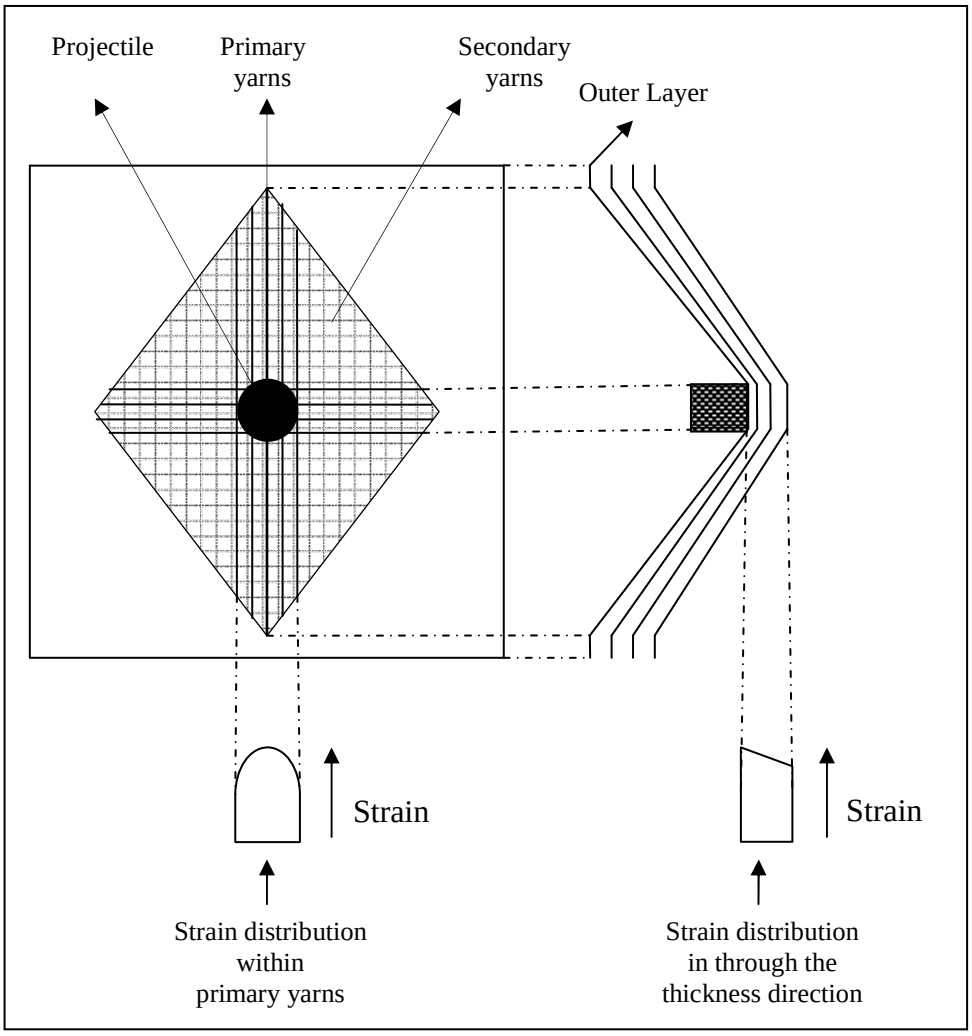

Figure 8. Representation of the Energy Absorption due to Pyramid Formation

2.9.2 Energy Absorption by Deformation of the Primary Yarns

Strain in the primary yarns results in some energy absorption. Strain in the primary yarns is higher than of the secondary yarns and these yarns fail under the tension that exceeds the maximum strain limit. Figure 8 shows that the strain variation in the primary yarns within a layer and between yarns in sequential layers.

The compression in the outer layers causes an extra straining where the strain would be maximized along the middle primary yarn in each layer. This is because the middle primary yarn is in contact with diameter of the projectile face whereas the other yarns are in contact with only the chord of the projectile face. So that each primary yarn in the system has a different strain rate. A particular primary yarn would fail when the strain of that particular primary yarn exceeds the maximum strain limit. There will be a sequential failure of the primary yarns starting within the top layer because of the strain variation in the system [31]. If the strain in the primary yarn is less than the strain limit, it would not be broken and the projectile would be caught.

The strain within the primary yarns is also varied along the radial direction and it is maximum at the point of impact with a lessening along the radial direction. Yarn failure would occur where the strain concentration is higher. Fabric and projectile geometry influence the strain concentration. For example, strain concentration would be present at the periphery of the projectile for a flat nose shape projectile where would be at the tip for a pointed projectile. There might be higher strain concentration distant from the impact point in certain practical situation, because of the geometry of the fabric and possible local imperfections.

2.9.3 Energy Absorption by Deformation of the Secondary Yarns

Energy absorption by the secondary yarns has two components: elastic strain and plastic deformation energy. The absorbed energy depends on the strain distribution within the secondary yarns and reduces linearly as one gets further from the impact point.

The total energy absorption by secondary yarns is more than the total energy absorption of primary yarns. This is because the number and the volume of the secondary

yarns is significantly more than that of the primary yarns. If the complete perforation of the target does not occur, the elastic strain energy would be transferred back to the projectile, and the projectile would rebound [31].

2.9.4 Energy Absorption due to Delamination

Energy absorption by delamination mechanism is minor compared to other energy absorbing mechanisms. As the longitudinal wave propagates along the yarns, stress wave reduction occurs. This causes strain variation which is at a maximum at the point of impact and zero strain at the location where the longitudinal stress wave has just reached.

Delamination takes place around the point of impact where the induced strain is above the damage strain limit for the material. Delamination continues until the complete perforation takes place, or the total energy of the projectile is absorbed by the target. During the ballistic impact event, delamination takes place before the yarn fractures. The delamination propagation on typical multi-ply systems is more along the warp and filling directions which is directed by the differences in material properties in different directions. As a result, the delaminated region appears in a quasi-lemniscate shape rather than a circular as shown in Figure 9 [32, 33].

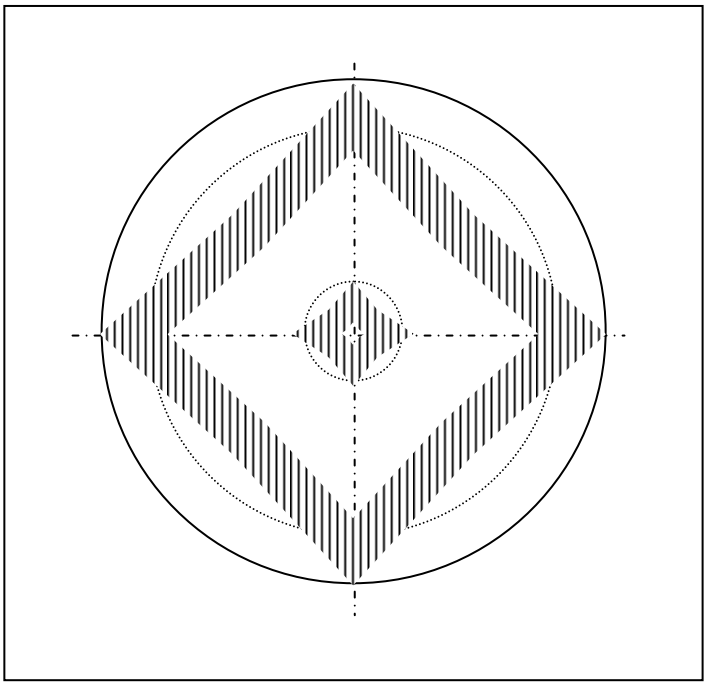

Figure 9. Shape of Delamination Region

2.9.5 Energy Absorption by Friction Mechanism

The projectile is subjected to frictional resistance during its sliding movement through fabric after tensile failure of the yarns. The frictional resistance depends on the parameters based on projectile and target structure. The parameters based on the projectile can be stated as projectile geometry and the friction coefficient between metal and the material under consideration. The parameters based on the target structure can be stated as the weave structure and material intrinsic properties such as stress-strain behavior, heat capacity and melting behavior. The friction between the yarns themselves may also contribute to the amount of the energy absorbed during the impact event. The projectile might get stuck in the target when its remaining energy is not sufficient to overcome frictional resistance. The energy absorbed by friction is converted into heat energy which results in a local temperature rise.

2.9.6 Energy Absorption Mechanism of Nonwoven Structures

Energy absorption mechanisms of nonwoven fabric have been investigated by numerous researchers but the complex ballistic response of nonwoven structures have not allowed a clear understanding of their behavior under ballistic impact. In the structures consisting of yarns, crossovers behave as partially fixed ends which a strain or wave is partially reflected and partially transmitted through [34]. As a result, in a woven fabric these crossovers increase the strain levels and allow the elongation in the yarn to reach its maximum which causes yarn breakage. Unidirectional structures have been developed to minimize the adverse effect of the crossovers by eliminating them. However, those cross-plied layers of unidirectional laid yarns still reflect part of the strain wave.

The energy absorption mechanism in a needle-punched fabric under ballistic impact is different from that of the woven fabrics or unidirectional structures where part of the impact energy is absorbed by breakage of the primary yarns. In addition, projectiles might cause lateral movement of the primary yarns by pushing them outside of the impact area and penetrate through the structure easily. In contrast, there would be few fixed crossovers in a needle-punched nonwoven fabric composed of relatively short staple fibers. The majority of the fibers have free ends while there are few fixed ends (made by crossovers) capable of reflecting the strain wave. As indicated in Section 2.7.6, the amplitude of the reflected strain wave from a free end has opposite direction to the amplitude of the original wave. Those waves tend to neutralize each other and cause the fiber's tensile stress to become zero behind the reflected wave front which does not allow the elongation of the fibers to exceed maximum strain limits. As a result it can be concluded that less fiber failure occurs in nonwoven structures under ballistic impact

compared to the woven and unidirectional structures. In addition, nonwoven fabric structure prevents lateral movement of the fibers easily due to their mechanically entangled complex structure [35]. In nonwoven materials, the modulus of the fibers is the most important property influencing into the ballistic performance [36].

2.10 The Amount of the Absorbed Energy in a Ballistic Impact Event

The amount of the absorbed energy could be calculated from the kinetic energy of a projectile that travels with a specific mass and velocity, with the conclusion that the total energy in the system is conserved while there is no external force acting on the system during ballistic impact event.

Ideally, it is the most demanding subject to be able to use a continuous measurement method of a projectile displacement and velocity change during a ballistic impact event. Ballistic impacts are highly sophisticated events, for the reason that parameters of a ballistic impact onto a system including large number of effects in accordance with intrinsic irregularities of the materials, and the matter becomes more complex with the hybrid systems at higher impact velocity. As a result, it is difficult to simulate numerically, or analytically, the ballistic behavior of the systems because of the complexity of damage mechanism. Much of the work, so far, has concentrated on developing empirical methods. However, empirical methods are based on a very high number of experimental results and not useful to solve particular problems. Until now, it has been difficult to construct realistic simulations which are applicable in different problems. It is much easier to obtain “before and after” impact data, to evaluate the performance of the structures under ballistic impact, such as the projectile impact velocity (V_i) and the projectile residual velocity (V_r).

The amount of the absorbed energy by the structure is regarded as the energy expended by the projectile in perforation event and, it can be calculated by subtracting the residual energy of the projectile from its initial impact energy. Therefore, above the ballistic limit,

$$E_{absorbed} = \frac{1}{2} m(V_{impact}^2 - V_{residual}^2)$$

In the non-perforated case, the amount of the energy absorbed by the fabric is taken as equal to the initial impact energy because the ballistic impact event occurs under ballistic limits and the lost projectile kinetic energy is completely absorbed by the fabric. Calculations can be done as follows while below the ballistic limit,

$$E_{absorbed} = \frac{1}{2} m V_{impact}^2$$

Where $E_{absorbed}$ (joules) is the energy absorbed by the fabric, m is the projectile mass (kg) and V_{impact} and $V_{residual}$ (m/s) are the impact and residual velocities, respectively.

In the ballistic events, energy absorption by the fabric usually displays three regimes as shown in Figure 10, those are below the ballistic limit, low velocity perforation and high velocity perforation regimes. Above the ballistic limits, energy absorption increase until a critical impact velocity after which it starts to drop marks the start of the high velocity perforation regime. Such high impact velocities show markedly more localized damage than low velocity perforations [27].

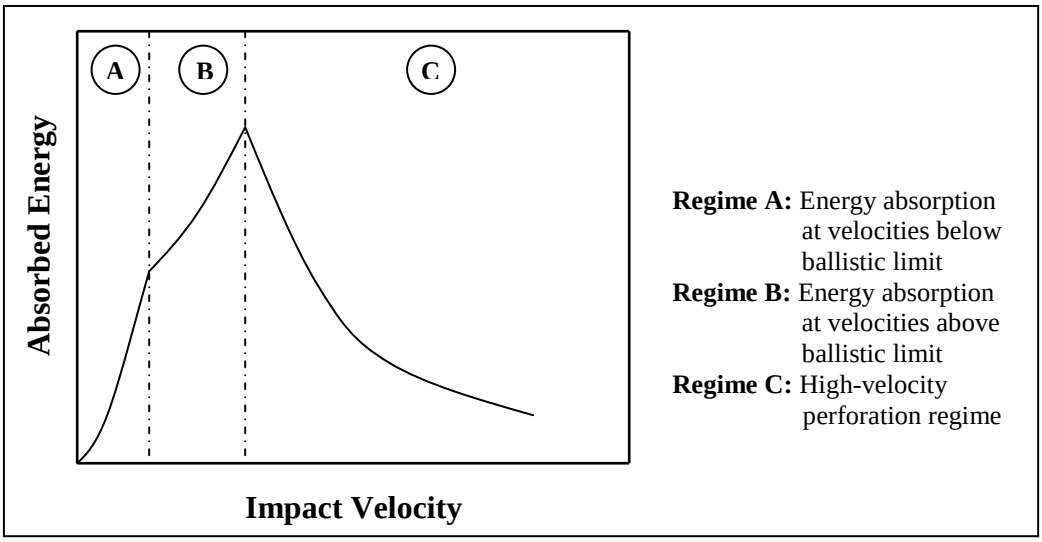

Figure 10. Fabric Energy Absorption due to Variable Impact Velocities

2.11 Equipment Standards for Ballistic Resistance of Personal Body Armor

The Office of Law Enforcement Standards (OLES) of the National Institute of Standards and Technology (NIST) developed NIJ Standard 0101.04 as an equipment standard for "Ballistic Resistance of Personal Body Armor" that is produced as part of the Law Enforcement and Corrections Standards and Testing Program of the National Institute of Justice (NIJ). NIJ Standard 0101.04 specifies the performance requirement that equipment should meet to satisfy the needs of criminal justice agencies for high quality service. The purpose of the standard is to establish minimum performance requirements and test methods for the ballistic resistance of personal body armor intended the torso against gunfire [37].

This standard classified personal body armor into seven categories according to their level of ballistic performance. The ballistic threat posed by a bullet depends on its composition, shape, caliber, mass and impact velocity. The test conditions specified in this standard represent general, common threats to law enforcement officers.

Ballistic resistant body armor suitable for full time wear during an entire shift of duty is available in classification Types I, IIA, II, and IIIA, indicated as in Table 1, which provide increasing levels of protection from handgun threats. Type IIIA armor is suitable for routine wear in many situations and provides the highest level of protection from high velocity 9 mm and 44 Magnum ammunition.

Table 1. NIJ Standard 0101.04 Classification

Threat Level	Caliber	Bullet Wt. (g/gr.)	Bullet Description	Bullet Dia. (nominal)
I	22 LR*	2.6/40	LRN	5.6 mm
	380 ACP	6.2/95	FMJ RN	9 mm
IIA	9 mm	8.0/124	FMJ RN	9 mm
	40 S&W	11.7/180	FMJ	10 mm
II	9 mm	8.0/124	FMJ RN	9 mm
	357 Mag	10.2/158	JSP	9.1 mm
IIIA	9 mm	8.0/124	FMJ RN	9 mm
	44 Mag	15.6/240	SJHP	10.9 mm
III	7.62 mm NATO	9.6/147	FMJ- SPIRE PT BT**	7.62 mm
IV	30.06 M2 AP	10.8/166	FMJ – SPIRE PT AP***	7.62 mm

* Commercially loaded ammunition may be used—handloading of this round is not required. See section 5.4.1.
** Verify that jacket is ferrous (use of a magnet is acceptable).
*** Obtained from U.S. Military M2 AP ammunition.

2.11.1 Baseline Ballistic Limit

The ballistic limit is an indication of a projectile's ability in defeating a target. It is defined as the velocity at which 50% of the impacts result in complete penetrations and 50% in partial penetrations according to the protection ballistic limit. Briefly, it is a statistical measure of the velocity at which penetration just occurs.

2.11.2 Penetration

Penetration of the projectile occurs in two forms: complete and partial penetrations. In the complete penetration (CP) form: perforation of an armor sample or panel by a test bullet or by a fragment of the bullet or sample itself, as evidenced by the presence of that bullet or fragment (armor or bullet) in the backing material, or by a hole which passes through the armor and/or backing material. In the second case, partial penetration (PP) form determined any impact that is not a complete penetration [37].

2.11.3 Backface Signature (BFS)

The depth of the depression made in the backing material, created by a non-penetrating projectile impact, measured from the plane defined by the front edge of the backing material fixture. For armor tested on built up or curved backing material, the BFS is measured from the plane defined by the top edges of the depression or pyramid formed by the impact. Complete penetration or any designated depth measurement of BFS in the backing material greater than 44 mm (1.73 in) constitute a failure.

CHAPTER THREE: METHODOLOGY

This chapter describes the materials that were subjected to tests, sample preparation and the methods of testing to gather data.

As a starting point, three different types of adhesive polymers: Poly (ethylene-co-acrylic acid), poly (ethylene-co-vinyl-co-acetate) and a polymer blend of low density poly (ethylene) with EVA, are investigated under shear and peel tests in an effort to simulate interlaminar response of the fabrics against the ballistic impact. Then, Drop-weight impact test was used as a preliminary investigation before the ballistic tests. Lastly, ballistic tests were done by four different types of bullet to investigate the velocity and the nose shape effect on the ballistic behavior of the systems.

3.1 Composition of the Materials

Two different types of woven fabrics and a needle-punched nonwoven fabric were used during the tests. Ballistic grade (BG) woven fabric, commonly used fabric for bullet proof vests, is constructed of 3100 denier Twaron® fibers in a plain weave (7x7 threads/cm) and a weight of 487.5 g/m^2. Knife proof grade (KPG) woven fabric is specifically designed for prison guards to prevent them from getting cut by sharp objects and relatively tighter than BG fabric. KPG fabric is constructed of 200 denier Twaron® fibers in a plain weave (28x28 threads/cm) and a weight of 125 g/m^2. The needle-punched nonwoven fabric is constructed by a blending of Kevlar® (K-29) and Spectra® fibers in a 50/50% ratio (b/w) at a weight of 85 g/m^2.

Three different types of adhesive polymers; poly (ethylene-co-acrylic acid) (EAA), poly (ethylene-co-vinyl-co-acetate) (EVA), and a polymer blend of low density poly (ethylene) and EVA (LDPE / EVA), was used during shear and peel tests. Properties of the polymers are summarized in Table 2.

Table 2. Specifications of Adhesive Polymers

Polymer	Brand / Type	Melting Point (^oC)	Thickness (μ)	Areal Density (g/m^2)
EVA	Conwed Plastic Inc.	108	100	95.4
EAA	Bloomer Plastic Inc. MC100H	110	70	51.2
LDPE/EVA	Bloomer Plastic Inc. BB900CJ	110	90	46.5

3.2 Sample Preparation for Shear and Peel Tests

KPG fabrics were used in shear and peel tests. The fabrics scoured in methanol and hexane before lamination to get rid of from any contaminants added during spinning and weaving processes. Two layers of KPG fabrics (25.4x127 mm) were laminated using a film of adhesive polymer that was treated in a heated press at 120 ^oC under 0.5 tons load for 20 minutes, as shown in Figure 11. Specimens for peel tests were laminated from alternating fabrics and film layers in the size of 25.4x101.6 mm (1x4 inch) while the specimens for shear test were in the size of 25.4x25.4 mm (1x1 inch), as shown in Figure 12.

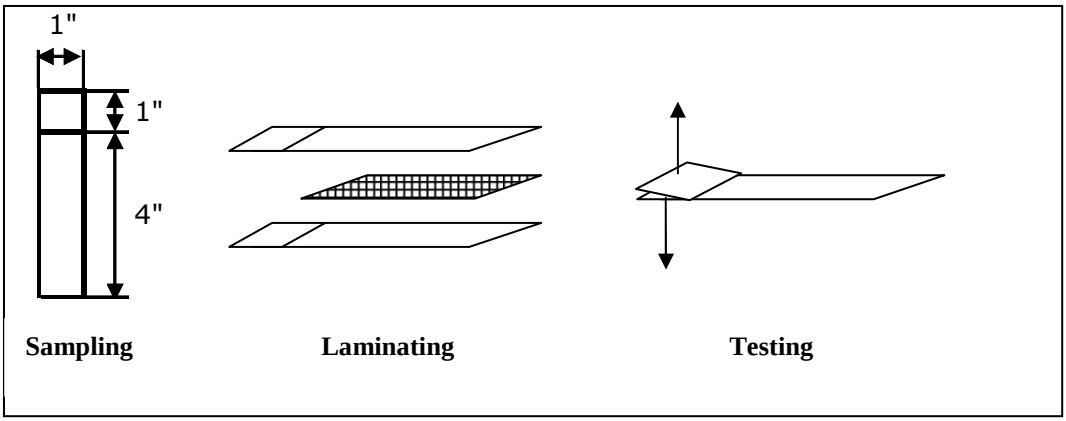

Figure 11. Representation of Sample Preparation and Testing for Peel Tests

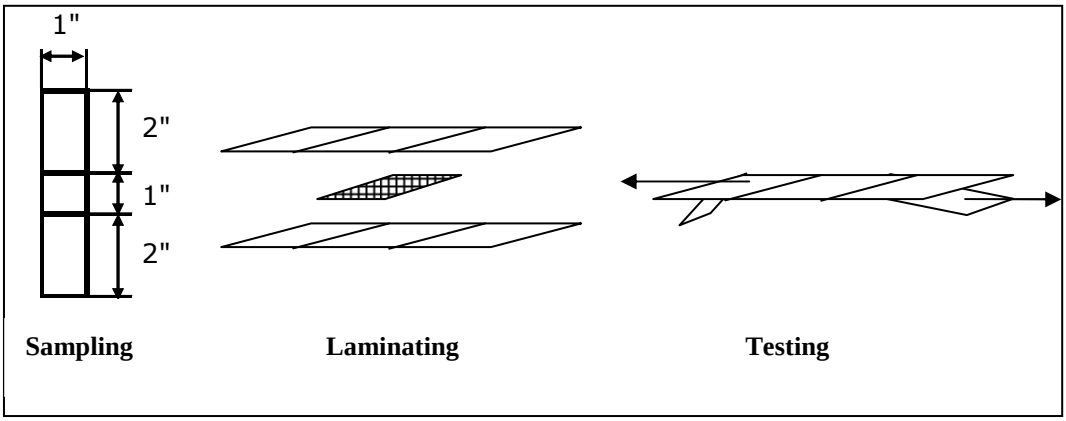

Figure 12. Representation of Sample Preparation and Testing for Shear Tests

3.3 Sample Preparation for Drop-Weight Impact and Ballistic Tests

Various numbers of woven and nonwoven fabrics were laminated according to designed experimental setups in the size of 114.3x114.3 mm (4½x 4½ inch) for the drop-weight impact tests. The fabrics scoured in methanol and hexane before lamination and were laminated by a film of adhesive polymer (114.3x114.3 mm) that is melted and pressed in a heated press at 120 ^{o}C under 0.5 tons load for 30 minutes.

Specimens for the ballistic tests were laminated in the size of 558.8x558.8 mm (22x22 inch) using a film of adhesive polymers in the size of 279.4x279.4 mm (11x11 inch) that is centered. The same procedure as in drop-weight impact tests was followed for the lamination process. For all pressing processes, two flat aluminum plates in the size of 279.4x279.4 mm (11x11 inch) were used on the lower and upper heater plates to ensure uniform pressure.

3.4 Experimental Setups

An Instron 4400R model II-22 was used to carry out the shear and peel tests. Pneumatic jaws (model no. 42-38) were used during the tests and covered with a fine grade of sand paper to avoid sample slippage. A tensile load cell Type CT was used for the tests. Tests were done with a 1270 mm/min. (50 inch/min.) jaw speed-the maximum speed of the instrument. Gauge length was set as 31.75 mm (1¼ inch) for the tests.

An Instron Dynatup 8250 drop-weight impact tester was used for the drop-weight impact tests. The tests were operated in the gravity mode by a free-fall of the crosshead. The crosshead weight was 5.41 kg. As shown in Figure 13, standard tip of the impact tester was modified by attaching a pointed tip to increase the effect of the impact action. The attached pointed tip had a 10mm diameter, 44mm length, 66.3g of weight and 90^{o} tip angle.

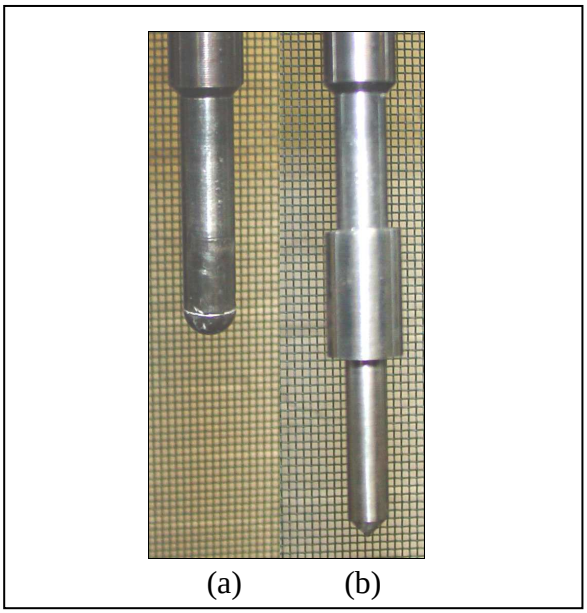

Figure 13. Standard (a) and Modified (b) Tip of the Drop-Weight Impact Tester

The velocity of the crosshead when operating in the gravity mode is determined analytically by the following equation;

$(v)^{1/2} = 2 \times g \times h$

where; v = theoretical velocity (m/sec)

g = acceleration of gravity (9.8 m/sec^2)

h = drop height (m)

The drop height was determined by 0.91m by adjusting the velocity detector. These setups let us to examine our samples with ~4.17 m/sec impact velocity and ~48 joules impact energy.

Two piece clamps were designed to avoid slippage which is a problem for the ballistic grade fabrics. The lower clamp, is shown in Figure 14, has a size of 152.4x152.4 mm (6x6 inch) with a centered impact hole of 76.2 mm (3 inch) diameter. Clamping quality was increased by three teeth, arranged around the impact hole with depth of 2mm,

width of 5mm and a gap of 5mm. A negative counterpart of the lower clamp is used for the upper side. Clamping force was provided by eight cap screws that are fastened through the 12.7 mm (1/2 inch) holes which are cut at the distance of 63.5 mm (2½ inch) from the center. An electric screwdriver was used to screw the cap screws to reach confident clamping pressures.

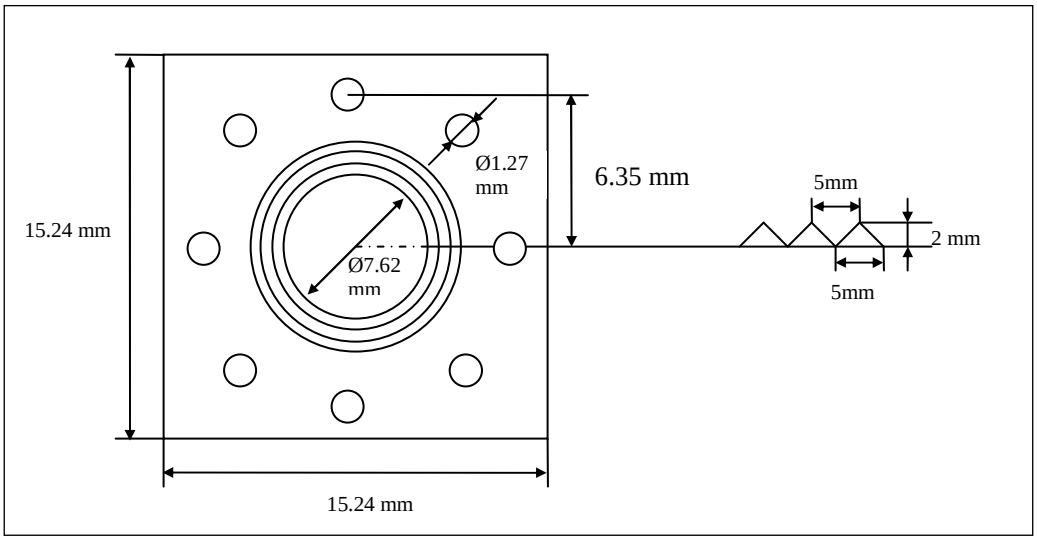

Figure 14. Top View of the Lower Clamp

For the ballistic tests, four different types of bullets were used as shown in Figure 15 with the specifications as summarized in Table 3. 22 caliber Short (a) and relatively faster 22 caliber High Velocity Short (b) round nose type of bullets were used to investigate low velocity impact behavior of the structures. 22 caliber Magnum Pointed (c) and Flat nose (d) bullets were used to investigate higher velocity impact behavior of the structures. In addition, bullet shape was used to create a shear effect (flat nose) and a slide-through effect (pointed nose).

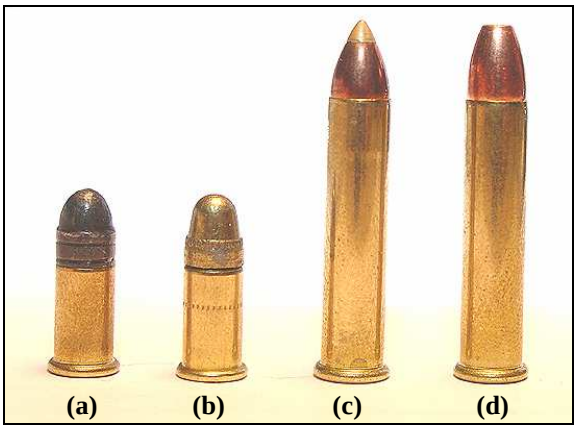

Figure 15. Bullets Used in Ballistic Tests

Table 3. Bullet Specifications Used in Ballistic Tests

Bullet Type	Brand	Bullet Weight (grains)	Nose Type	Measured Average Initial Velocity (m/s)
22 cal. Short	CCI .22 Short	29	LRN *	144
22 cal. Short HV	Remington .22 Rimfire HV	29	PLRN **	255
22 cal. Magnum Pointed	Remington 22 Win Mag	33	AccuTip-V	369
22 cal. Magnum Flat	CCI Maxi-Mag	40	TMJ ***	318

* lead round nose, ** plated lead round nose, *** totally metal jacket

Most of the measurement systems, currently used, are inadequate to make simultaneous measurement of the bullet velocity during ballistic events. The most commonly used systems are high-speed photography, chronographs and optical sensors. Two Oehler Model 35 Proof chronographs were used in the ballistic tests. The chronographs had a 4.0 MHz oscillator for 0.25 microsecond time resolution [38]. With

these measurement systems, the velocity is calculated from the known distance between two sensors divided by the time taken for the bullet to travel between the two light sensors.

Samples were clamped between two square alloy iron clamps, with a sufficient pressure using C clamps and placed on a support table. Shootings were performed from a distance of 4.57 m (15 feet) to the target and 3.51 m (11½ feet) to the initial velocity chronograph, as shown in Figure 16. Initial and post-target chronographs were placed with a distance of 0.46 m (1½ feet) from the target.

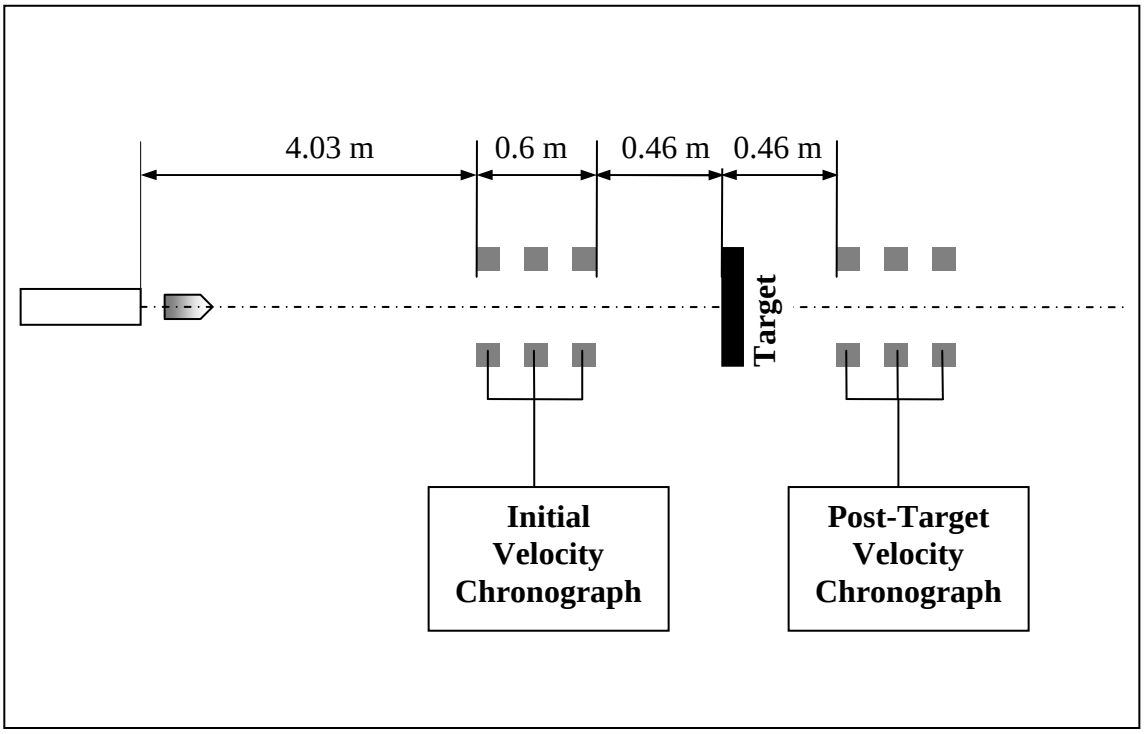

Figure 16. Experimental Setup for Ballistic Tests

CHAPTER FOUR: RESULTS AND DISCUSSION

This chapter presents the results of Shear and Peel, Drop-Weight, Ballistic, Microscope and Postmortem tests. The results were analyzed and interpreted in accordance with their effect on the research objectives.

4.1 Shear and Peel Test Results

EAA, EVA and LDPE/EAA blend films were subjected to shear and peel tests to simulate their possible response during impact action. As a starting point, three different groups of samples were prepared to investigate the effect of contamination on the adhesion efficiency of the films. Samples were prepared by the KPG fabrics, those are untreated, washed in methanol and hexane (respectively), and scoured in 70 ^{o}C distilled water.

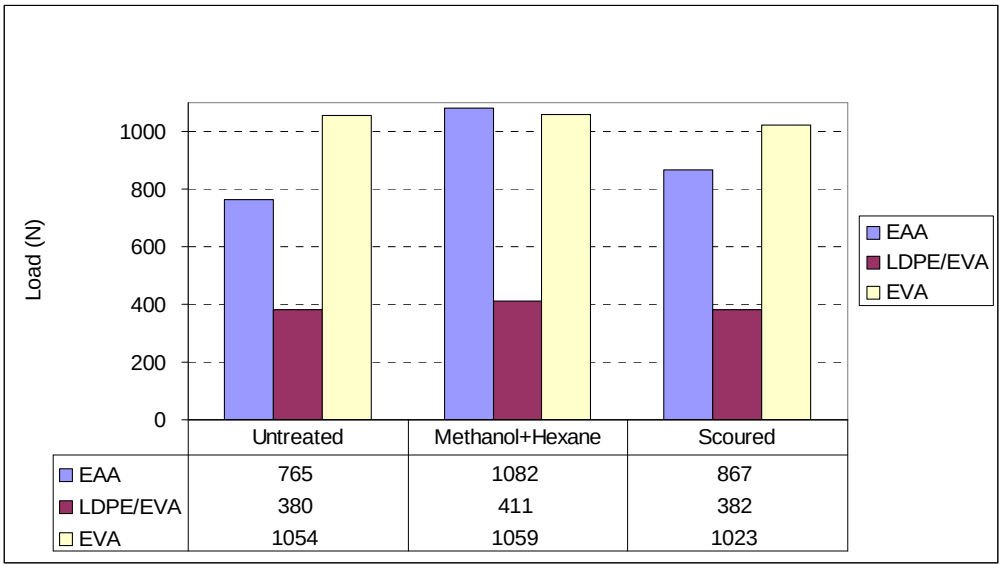

Figure 17. Results of Shear Test

As shown in Figure 17, it has been observed that the higher adhesion efficiency can be provided by washing the fabrics in methanol and then hexane before the lamination process.

As concluded from the data of adhesion efficiency tests, only the solvent washed samples are reported for shear behavior of the polymer films shown in Figure 18. EAA and EVA films showed higher performance in the shear test compared to LDPE/EVA blend film. EAA and EVA films performance in the shear test are similar. However, it can be concluded that EAA film has a better performance than EVA film based on weight/performance ratio with the areal densities those are 51.2 gsm and 95.4 gsm, respectively. Additionally, all of the polymer films performed strain values in a narrow gap between 18-25%.

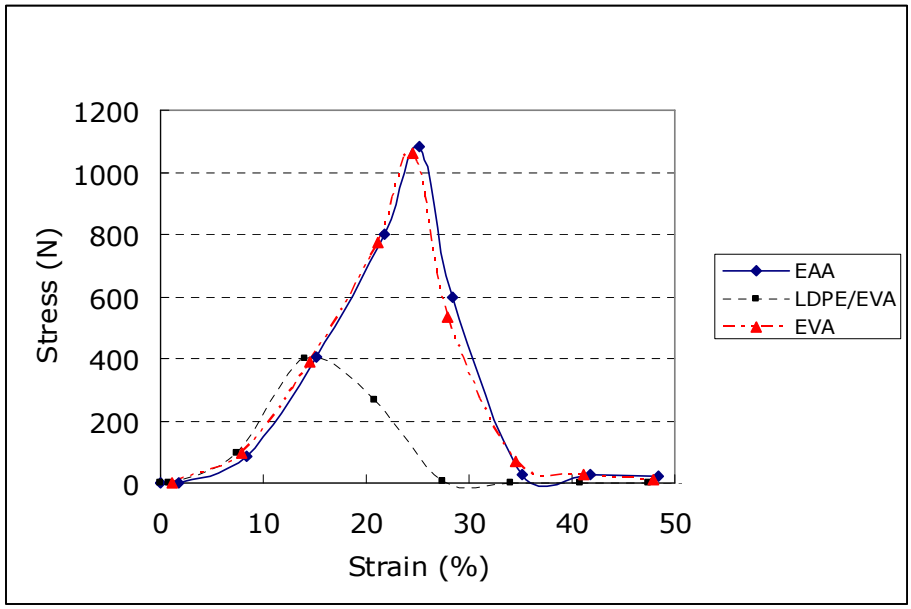

Figure 18. Shear Behavior of the Polymer Films

As shown in Figure 19, EAA and EVA were also two candidates for the best performance in the peel tests. At first, it seemed the EVA film performed better in peel test but it has been determined that a more appropriate evaluation could be done by the normalization of the results. The glue strength results were normalized by the division of the average load values by the film areal densities. In conclusion, EAA film had a value of 0.223 (Nxm^2/g) while EVA was 0.213 (Nxm^2/g) which indicated that, on a weight basis, the EAA film had higher performance in the peel test as in shear test. We therefore chose to use EAA adhesive polymer during our drop-weight impact and actual ballistic tests.

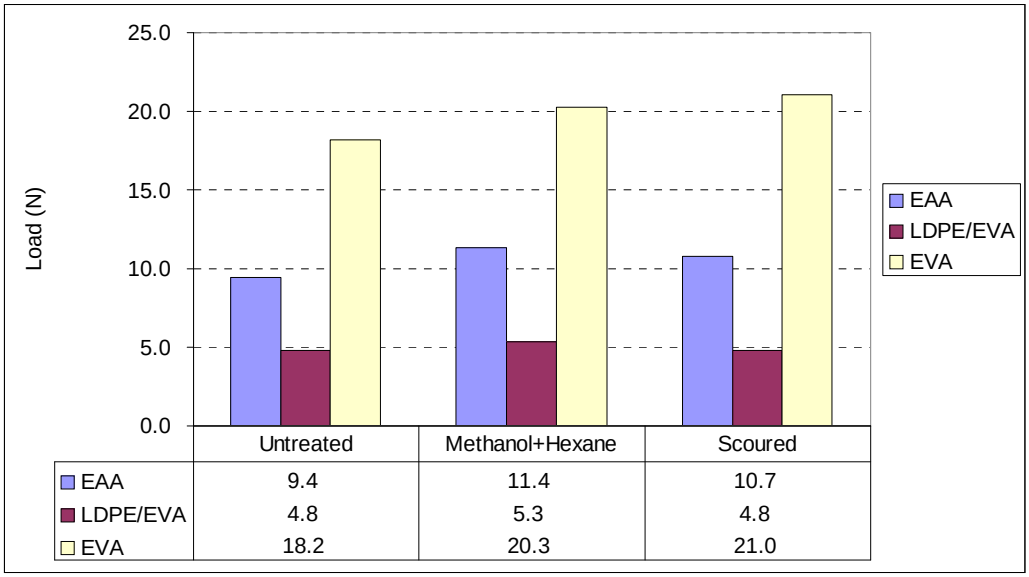

Figure 19. Result of Peel Tests

4.2 Drop-Weight Impact Test Results

A single layer of EAA polymer film was used to laminate the impact test samples, as concluded from the shear and peel tests. Seventeen different sample groups, as shown in Table 4, were subjected to drop-weight impact test to investigate performance of the lamination and nonwoven fabric usage on the outer (impact) side.

Table 4. Composition of the Samples for Drop-Weight Impact Test

Sample No.	Composition of the Material (Inner to outer)	Areal Density (g/m^2)
1	1 BG	487.5
2	2 BG	975.0
3	3 BG	1462.5
4	1 BG + EAA + 1 BG	1026.2
5	2 BG + 1 NW	1060.0
6	2 BG + 2 NW	1145.0
7	2 BG + EAA + 1 NW	1111.2
8	2 BG + EAA + 2 NW	1196.2
9	1 BG + EAA + 1 BG + 1 NW	1111.2
10	1 BG + EAA + 1 BG + 2 NW	1196.2
11	1 BG + EAA + 1 BG + EAA + 1 NW	1162.4
12	1 BG + EAA + 1 BG + EAA + 2 NW	1247.4
13	1 KPG	125.0
14	2 KPG	250.0
15	3 KPG	375.0
16	4 KPG	500.0
17	8 KPG	1000.0

BG: Ballistic grade woven fabric, NW: Nonwoven fabric, EAA: Poly(Ethylene-co-acrylic acid) film

Samples #1, #2 and #3 provided information about characteristic impact behavior of layered ballistic grade fabric. They also allow us to make comparisons and further investigation on the performance of the lamination and nonwoven facing usage based on their areal density.

Table 5. Drop-Weight Impact Test Results

Sample No	Impact Energy (joule)	Impact Velocity (m/sec)	Max. Load (kN)	Energy to Max. Load (joule)	Total Deflection at Failure (calculated) (mm)	Total Time (msec)	Total Absorbed Energy (joule)
1	46.35	4.18	1.82	11.43	14.56	3.68	13.86
2	47.64	4.17	2.86	19.94	18.48	4.97	25.33
3	46.07	4.18	3.30	31.98	19.92	6.03	37.84
4	47.61	4.17	3.90	29.55	19.12	5.46	35.04
5	47.72	4.17	3.43	23.41	17.22	4.74	29.21
6	47.66	4.17	2.74	22.44	24.63	7.42	31.17
7	47.58	4.17	4.26	30.15	18.26	5.21	35.63
8	47.60	4.17	3.78	32.05	24.40	8.38	41.11
9	47.62	4.17	3.42	32.53	23.47	7.34	38.83
10	47.60	4.17	2.91	32.45	26.36	8.51	40.40
11	47.51	4.16	4.11	37.18	22.07	8.56	47.51
12	47.53	4.17	4.02	37.90	21.68	8.50	47.08
13	46.96	4.17	0.25	0.93	9.31	2.05	1.47
14	45.59	4.16	0.52	1.19	9.78	2.22	2.52
15	45.88	4.17	0.76	3.68	10.95	2.67	4.64
16	45.92	4.17	1.16	3.01	11.85	2.85	6.96
17	45.78	4.16	2.91	13.51	15.45	4.04	21.18

Sample #4 was designed to get information about the performance of the lamination, but the maximum energy capability of the instrument did not allow us to test a three layer laminated sample. This handicap was eliminated by a comparison of the performance differences between samples #5 and #6 with the laminated samples #9 and #10. Samples #7, #8, #11 and #12 were designed to investigate the efficiency of sticking the nonwoven layer on the outer surface. Samples #13 through #17 provided information about impact behavior of knife proof grade fabric.

As shown in Figure 20, total energy absorption of single and multi layers of BG fabric exhibited a trend, characterized as a linear function “y = mx”, where the slope (m) had a value of 0.0246. By the known slope, the expected total energy absorption of the layered BG fabrics could be calculated at a given areal density. Then, the performance of the lamination and the nonwoven facing usage could be interpreted.

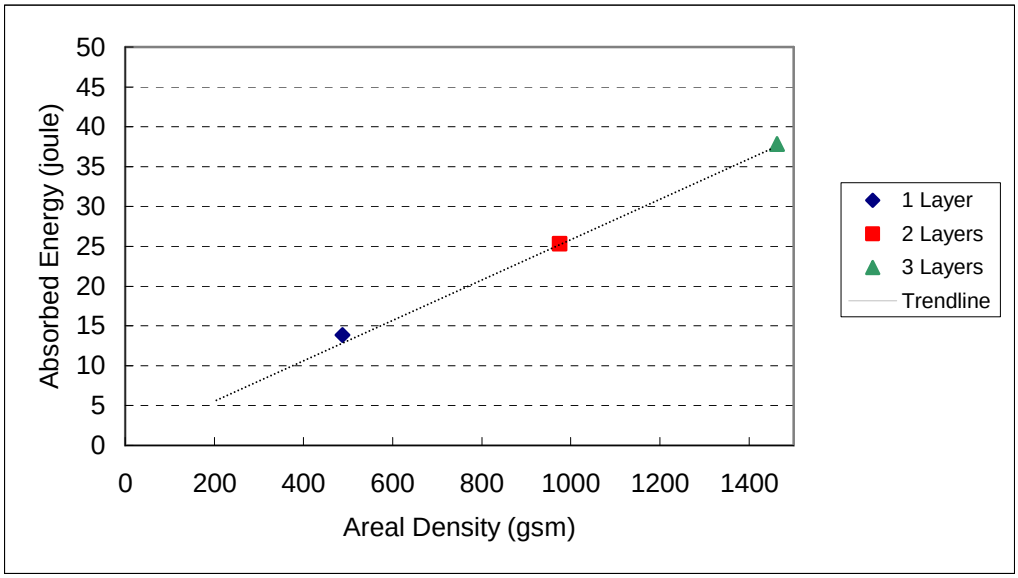

Figure 20. Energy Absorption of Single and Multi Layer BG Fabrics

Knife proof grade fabric showed much worse performance than the ballistic grade fabric as expected, shown in Figure 21. One layer of KPG fabric absorbed 9.4 times less impact energy than BG fabric. It is obvious that multiple KPG fabric layers are less effective than BG fabrics at the same weight. The combination of KPG fabric in front of BG fabric, however, is synergistic in its effect and provides much greater energy absorption. Both BG and KPG plots showed linear trendlines intersecting the origin (x_0=0, y_0=0) that prove no energy absorption at zero mass target.

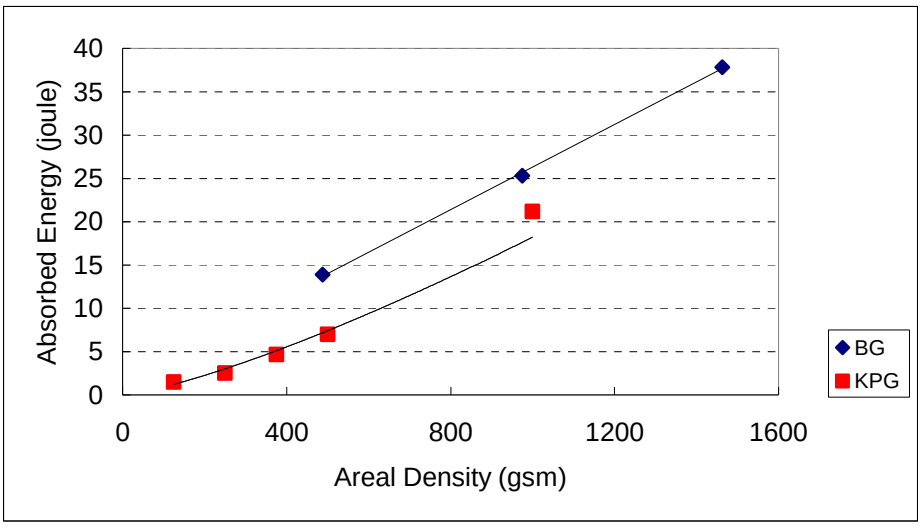

Figure 21. Energy Absorption of Single and Multi Layer KPG Fabrics

As shown in Figure 22, 2 layers laminated structure became slightly heavier because of the added adhesive, is not very strong, and exhibited 39% higher energy absorptions based on its areal density. Adhesive EAA film restricted the lateral movement of the primary yarns and made the sliding-through movement of the tip difficult between the primary yarns.

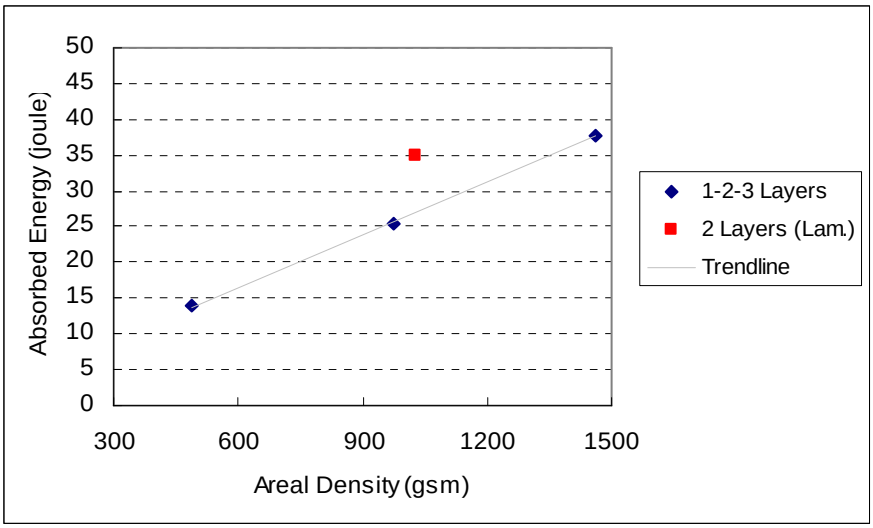

Figure 22. Energy Absorption of Laminated BG Fabrics

A comparison between the samples #5 and #6 and the samples #9 and #10, presented in Figure 23, also indicated an increase in the performance of the impact behavior through lamination. For the low velocity impacts, indirect effect of the lamination on ballistic performance can be seen easily while further investigation is needed for high velocity impact behavior.

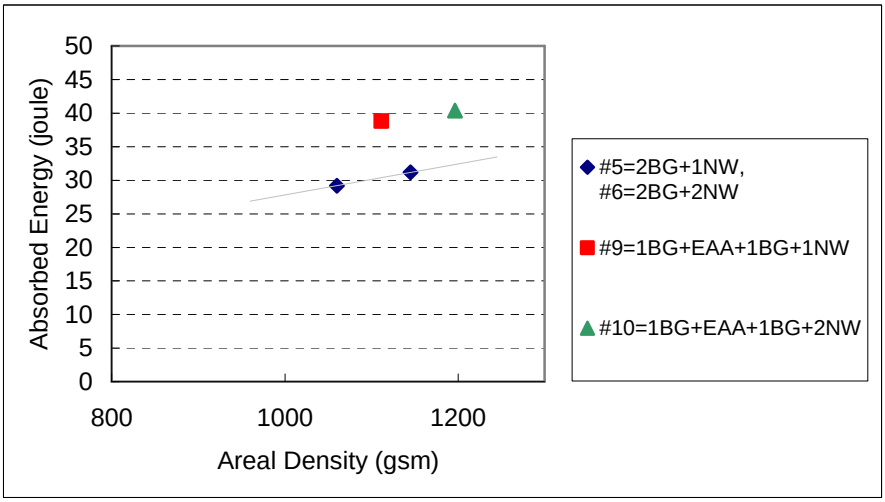

Figure 23. Energy Absorption of Laminated BG Fabrics Hybridized with Outer Nonwoven Layer

Nonwoven facing usage on the impact side (sample #5) improved energy absorption by 4%, as shown in Figure 24. The improvement can be explained by the movement of the nonwoven layers with the tip through the inner layers that causes a higher abrasion friction surface and perhaps a higher diameter. It has been observed that the 2nd layer nonwoven did not improve the impact behavior (sample #6) when compared with the single layer usage as in sample #5. Post-impact observations also indicated that nonwoven layer moves with the tip through inner layers, as shown in Figure 25.

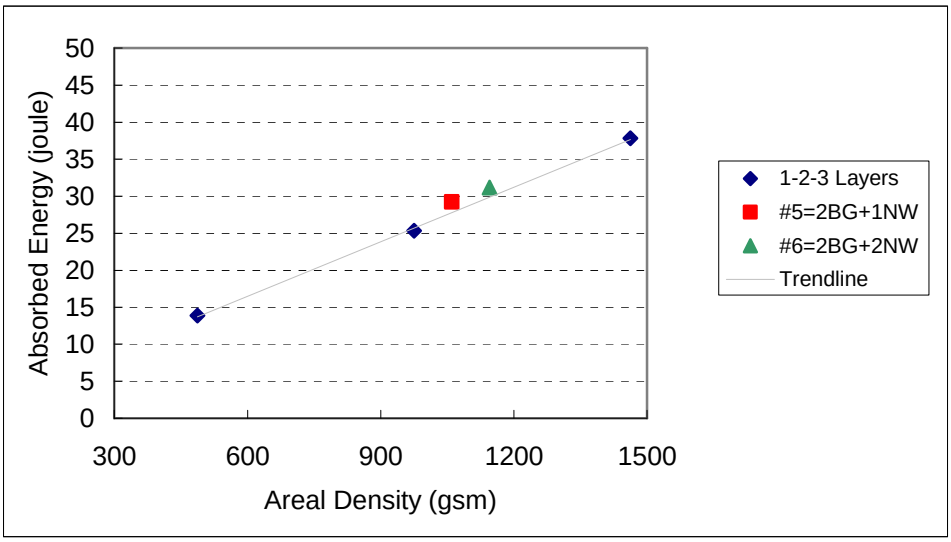

Figure 24. Energy Absorption of Nonwoven Facing

Figure 25. Nonwoven Layer Movement through Inner Layers

As shown in Figure 26, energy absorption of the designed structures had higher performance based on their areal densities. EAA adhesive lamination exhibited a higher performance when used between BG fabrics (sample #9), rather than between BG fabric and nonwoven facing (sample #7). It could be explained by the earlier breakage of the fibers inside the constrained nonwoven layer resulted in the loss of their abrasive effect. This behavior found an answer with an improvement in the energy absorption (9.4%) by an additional non-laminated outer nonwoven layer as in sample #8 compared to sample #7. The disadvantage of the lamination of nonwoven facing disappeared when an additional nonwoven layer was used. Sample #9, #10, #11 and #12 also exhibited performance advancing by lamination and nonwoven fabric usage. Sample #12 exhibited less performance when compared to sample #11 for the reason that absorbed energy reached the maximum energy capacity of the test instrument.

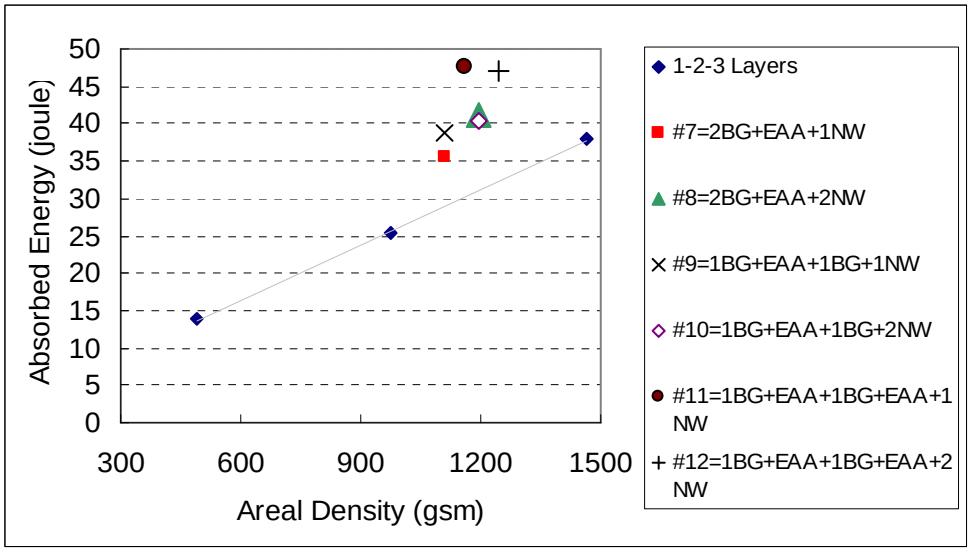

Figure 26. Comparison of Fabric-Fabric Lamination vs. Fabric-Nonwoven Lamination

4.3 Ballistic Test Results

Fifteen groups of samples were prepared for the ballistic tests within specifications, summarized as in Table 6, that were anticipated to have supportive information on the research. Most of the groups were designed to reveal the behavior of adhesive lamination and the nonwoven facing usage on the impact side. The rest of the designs were prepared to identify some other parameters for further research.

Table 6. Composition of the Samples for the Ballistic Test

Sample No.	Composition of the Material (Inner to outer)	Areal Density (g/m^2)
1	1 BG	487.5
2	1 BG +1 NW	572.5
3	2 BG	975.0
4	1 BG + EAA + 1 BG	1026.2
5	2 BG + 1 NW	1060.0
6	1 BG + EAA + 1 BG + 1 NW	1111.2
7	3 BG	1462.5
8	1 BG + EAA + 1 BG + EAA + 1 BG	1564.9
9	3 BG + 1 NW	1547.5
10	1 BG + EAA + 1 BG + EAA + 1 BG + 1NW	1649.9
11	1 NW + 3 BG + 1 NW	1632.5
12	1 BG + 1 KPG + 1 NW	697.5
13	2 BG + 1 KPG + 1 NW	1185.0
14	1 BG + EAA + 1 NW + 2 EAA + 1 NW + EAA + 1 BG	1349.8
15	1 BG + EAA + SAND + EAA + 1 BG + EAA + SAND + EAA + 1 BG	2147.3

Samples #1 to #11 were subjected to ballistic tests to investigate the performance of lamination and nonwoven layer usage on the impact side. Samples #1, #3, and #7 allowed us to gather characteristic information about the ballistic behavior of BG fabrics and offer data to evaluate the performance of the designed structures. Samples #2, #5, and #9 were tested to evaluate the performance of the nonwoven facing on the impact side, but nonwoven layers were not laminated on to the system because of their poor efficiencies as determined through drop-weight impact tests. Samples #4 and #8 were tested to evaluate the performance of lamination, and samples #6 and #10 for the both purposes.

Samples #12 and #13 were prepared to investigate the efficiency of knife proof grade (KPG) fabric which is relatively tighter than BG fabrics. Sample #14 was prepared to evaluate the performance of a nonwoven layer which is highly penetrated by the adhesive and assumed to be behaved as a 3D composite structure. Lastly, sample #15 was prepared to examine the effect of sand particles that are scattered between the BG fabric layers. It was assumed that sand particles would cause some energy absorption by fragmentation during ballistic impact event.

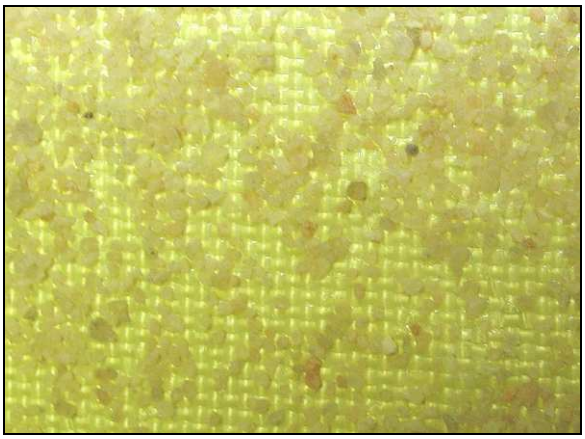

Figure 27. Sand Scattering between BG Fabrics

Table 7. Ballistic Test Results

Sample No	Absorbed Energy (joules)			
	.22 Short	.22 Short HV	.22 Magnum Sharp	.22 Magnum Flat
1	2.39	3.82	4.10	9.38
2	13.46 **	11.27	0.40	4.94
3	5.90	13.97		13.60
4	5.72	21.46	9.59	17.34
5	14.28 ***	20.56	2.97	12.99
6	14.08 **	36.41		21.07
7	11.77	32.49		26.75
8		65.29 **		25.25
9		30.62		24.58
10	20.41 +	67.78 +	9.30	36.29
11				34.97
12	20.85 +	34.76		
13		49.76 *		37.34
14		68.23 +		22.56
15		61.31 *		15.61

* One bullet stop, ** Two bullets stop, *** Three bullets stop, + All bullets stop.

As shown in Figure 28, the highest energy absorptions by the structures occurred within the 0.22 Short HV bullet shots because of the relatively higher initial kinetic energy than the 0.22 Short and non-cutting effect compared to the 0.22 Magnum

Flat Nose bullets. Tests with the 0.22 Magnum Sharp Nose bullet were stopped after shooting few targets because of variable results that was assumed to result from the extreme penetration influence which generated a narrow data range that could not be analyzed.

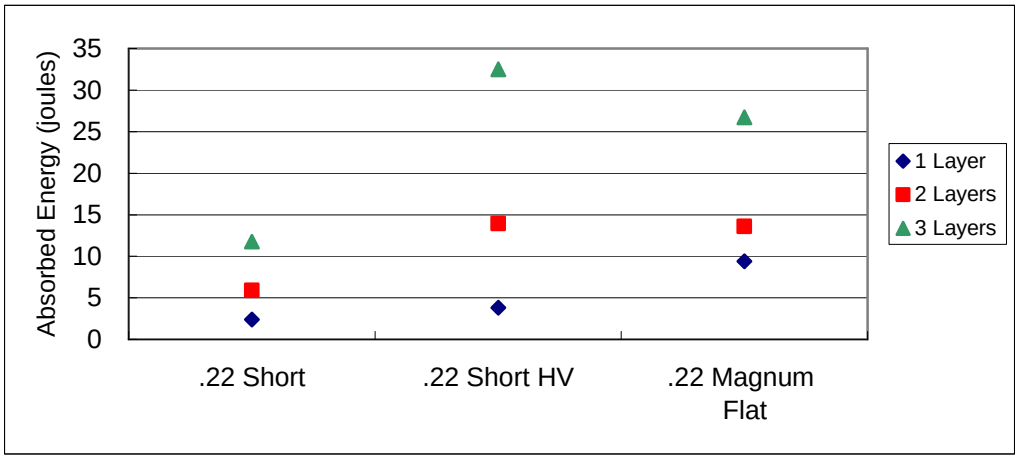

Figure 28. Ballistic Behavior of the BG Fabrics

Ballistic performance of the laminated structures is evaluated by comparison with the unlaminated structures. As shown in Figure 29, 0.22 Short bullet results did not offer reasonable results because the high incidence of caught bullets resulted from the complete energy absorption. Ballistic performance was obviously increased by the lamination within the 0.22 Short HV shots whereas a decreasing performance observed for the 0.22 Magnum Flat Nose shots. This behavior could be explained by increasing cutting effect of the flat nose bullets on the outer layers as a result of the limitation on the yarn movements by the adhesive which is being worsened by the compressive support of the inner layers. These conclusions could be investigated more equably by making comparisons on the weight/performance base, as shown Figure 30, and Figure 31.

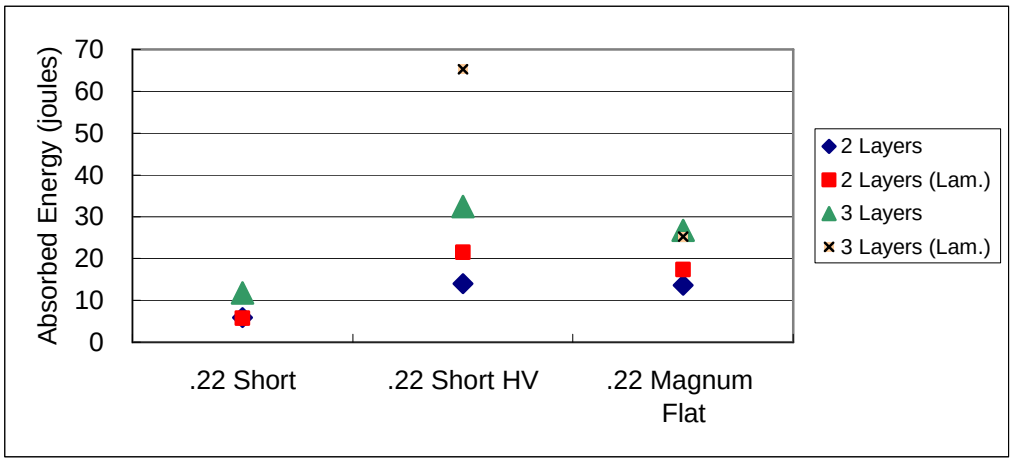

Figure 29. Ballistic Test Results of Laminated Structures

As shown in Figure 30, two-layer laminated structure showed 33% higher performance and three-layer laminated structure showed 78% higher performance due to lamination, under ballistic tests with 0.22 Short HV bullets.

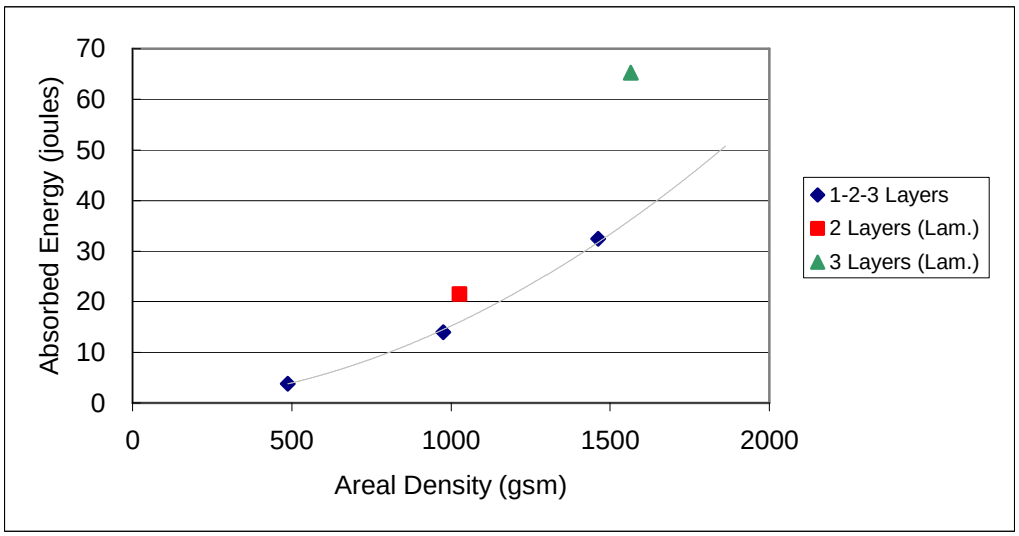

Figure 30. Ballistic Test Results of Laminated Structures II(0.22 Short HV)

According to flat nose bullet tests, Figure 33, also confirmed an increasing in the ballistic performance (6%) due to lamination by the results of sample #4 (two layers laminated) while sample #8 (three layers laminated) lost its efficiency (8%).

However, the cutting effect, reasonably explained in the previous section, was reduced by using a nonwoven facing as in sample #6 and #10. Ballistic performance of these structures increased 15% and 27%, respectively. This case could be explained by the freely moving fibers in the nonwoven structure lessening the cutting effect of the flat nose.

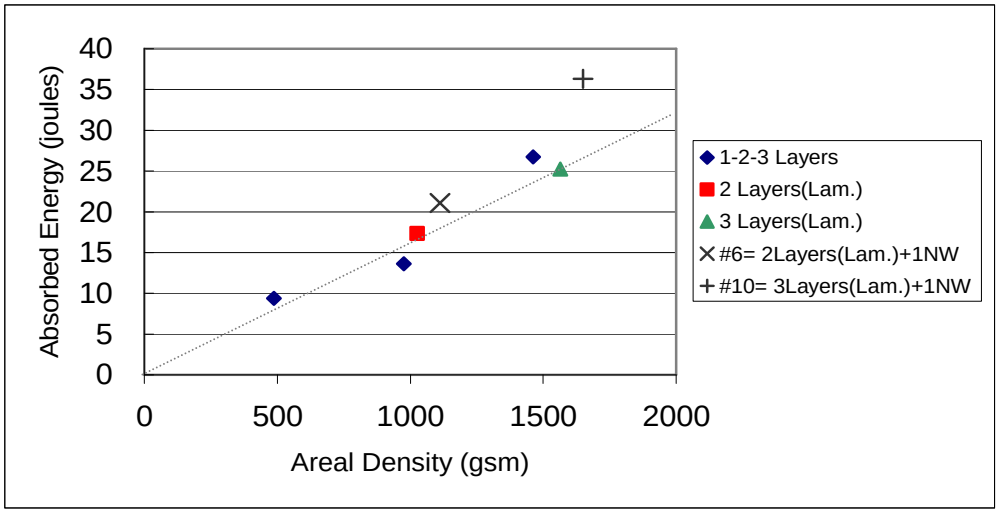

Figure 31. Ballistic Test Results of Laminated Structures III (0.22 Magnum Flat Nose)

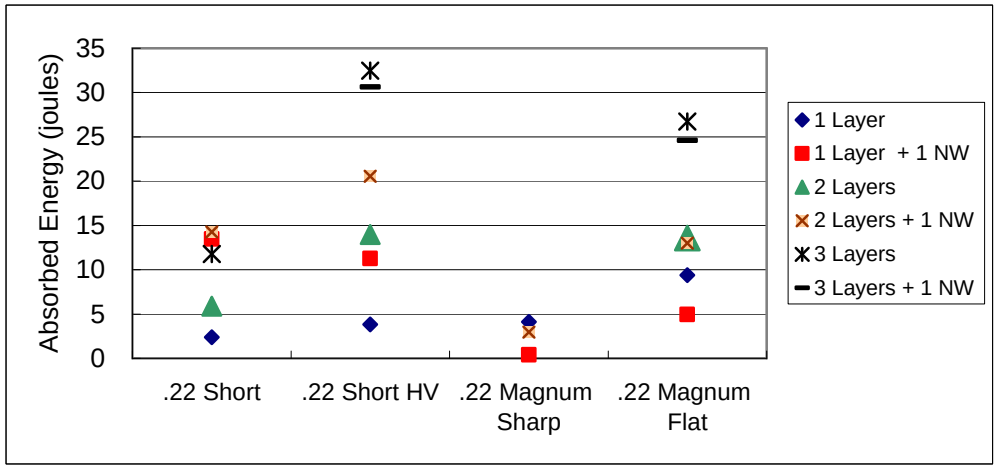

Figure 32. Ballistic Test Results of Nonwoven Facing Usage I

Performance of nonwoven facing usage on the impact side, using 0.22 short HV bullet tests, is shown in Figure 33. The performance showed an increase for one layer (116%) and two layers (19%) and a declining trend through the increasing areal density. Nonwoven layer on the outer layer lost its efficiency (15%) when used with three layers of BG fabric.

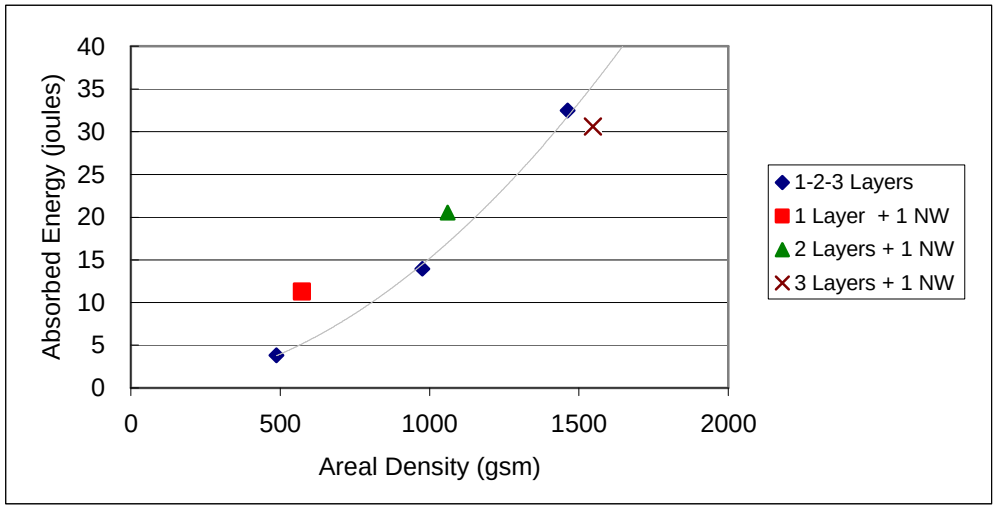

Figure 33. Ballistic Test Results of Nonwoven Facing Usage II (0.22 Short HV)

As shown in Figure 34, nonwoven facing exhibited worse performance for all samples through the 0.22 Magnum Flat Nose bullet ballistic tests. Sample #2 (1layer+1NW), Sample #5 (2layers+1NW) and Sample #9 (3layers+1NW) lost their efficiencies by 50%, 23% and 15%, respectively. That behavior might be explained by the slide-through effect that is lubricated by broken fibers in the nonwoven layer. Fiber breakages are increased by the flat nose high velocity magnum bullets.

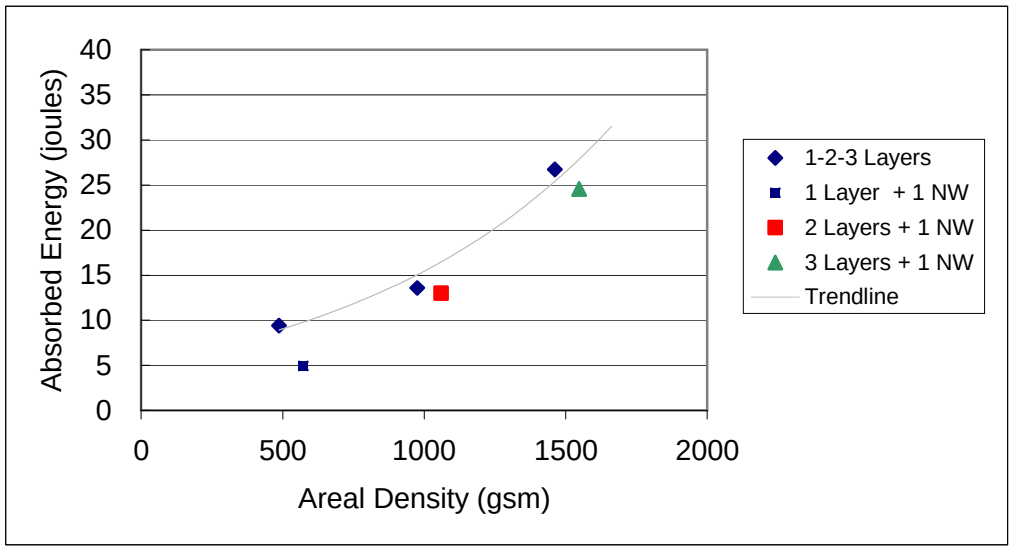

Figure 34. Ballistic Test Results of the Nonwoven Facing Usage III (0.22 Magnum Flat Nose)

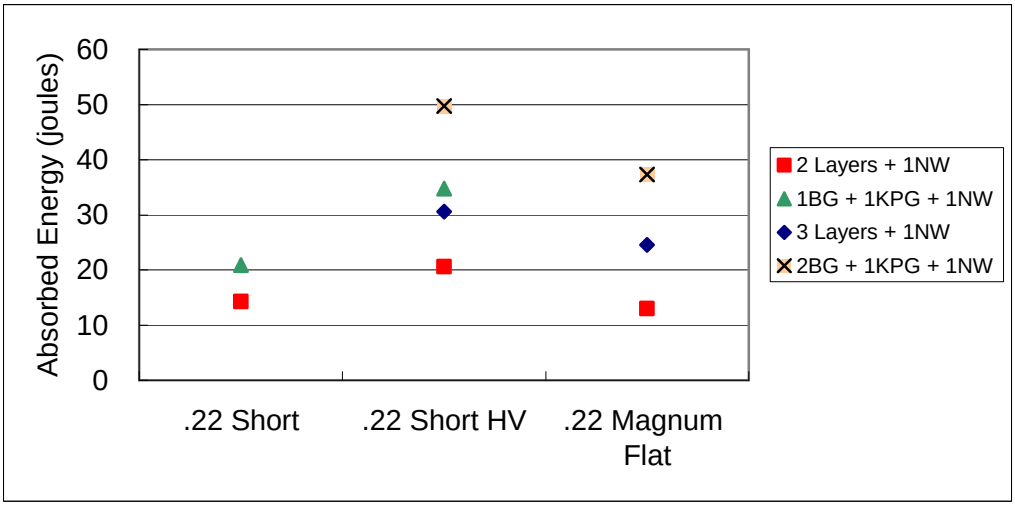

Figure 35. Ballistic Test Results for Compositions Containing KPG Fabrics I

Knife proof grade (KPG) fabrics significantly increased the ballistic performance of the structures, in the ballistic tests with both 0.22 Short HV and 0.22 Magnum Flat Nose bullets, beside their light weight structures. Further investigations

based on the weight/performance ratio also showed significant enhancements as seen in Figure 36 and 37.

Figure 36 shows the total energy absorption of single and multi layers of BG fabric in 0.22 Short HV tests exhibited a trend which can be characterized as a power function " $y = 2.33x10^{-5}\ x^{1.94}$ ". One layer of KPG grade fabric improved the energy absorption by 350% when used between one layer of BG fabric and a nonwoven layer, and by 130% when used between two layers of BG fabric and a nonwoven layer. These improvements in energy absorption can be explained by the prevention of slide-through motion of the bullets by the tightly woven KPG fabrics, noting that KPG fabric can not absorb higher energy by itself as reported during the drop-weight impact tests. In conclusion, KPG fabrics offered the possibility to primary yarns of the sequenced BG fabrics to absorb more energy.

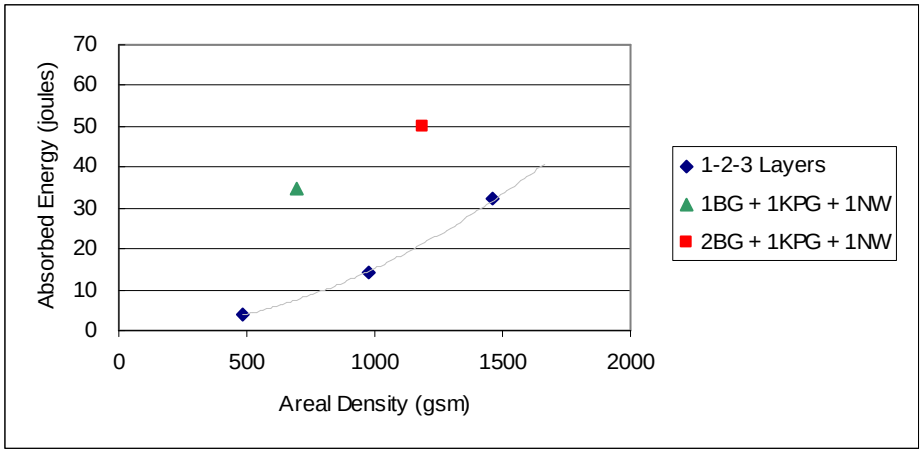

Figure 36. Ballistic Test Results for Compositions Containing KPG Fabrics II (0.22 Short HV)

Total energy absorption of the single and multi layers of BG fabric, in 0.22 Magnum Flat Nose bullet tests, exhibited a trend which can be characterized as a exponential function “y = 0.0178x”. One layer of KPG fabric improved the energy absorption by 84% when used between two layers of BG fabric and a nonwoven layer. Usage of the KPG fabric also eliminated the potential slide-through effect of the nonwoven layers as discussed in the previous section. Usage of the KPG fabrics also allowed an achievement, which could not be provided by using nonwoven facing alone; the cutting effect of the flat nose bullets was reduced while avoiding the slide-through disadvantage of the nonwoven layers.

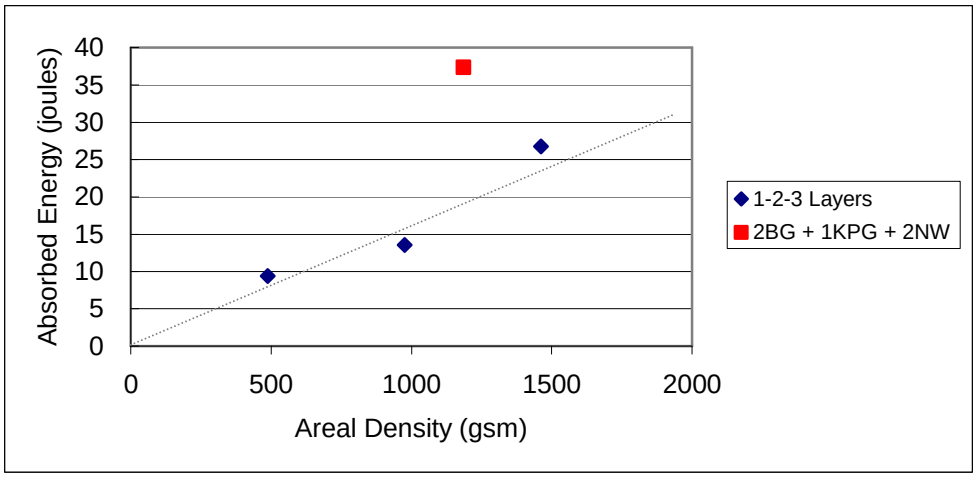

Figure 37. Ballistic Test Results for Compositions Containing KPG Fabrics III (0.22 Magnum Flat Nose)

The data of the designed structures for further research is presented in Figure 38, and Figure 39. Composite structure (#14) exhibited higher energy absorption (54%) due to ballistic impact with 0.22 Short HV bullets while there is no effect in the ballistic tests with 0.22 Magnum Flat nose bullets. Nonwoven fabrics also increased the energy

absorption through the tests with round nose bullets when we laminate them between the layers.

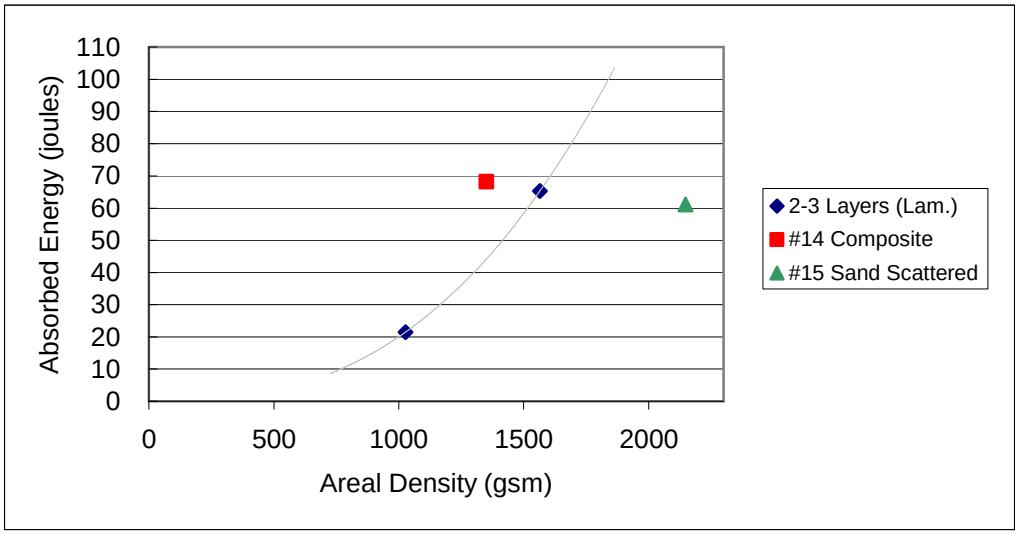

Figure 38. Ballistic Test Results of the Composite and Sand Scattered Structures I (0.22 Short HV)

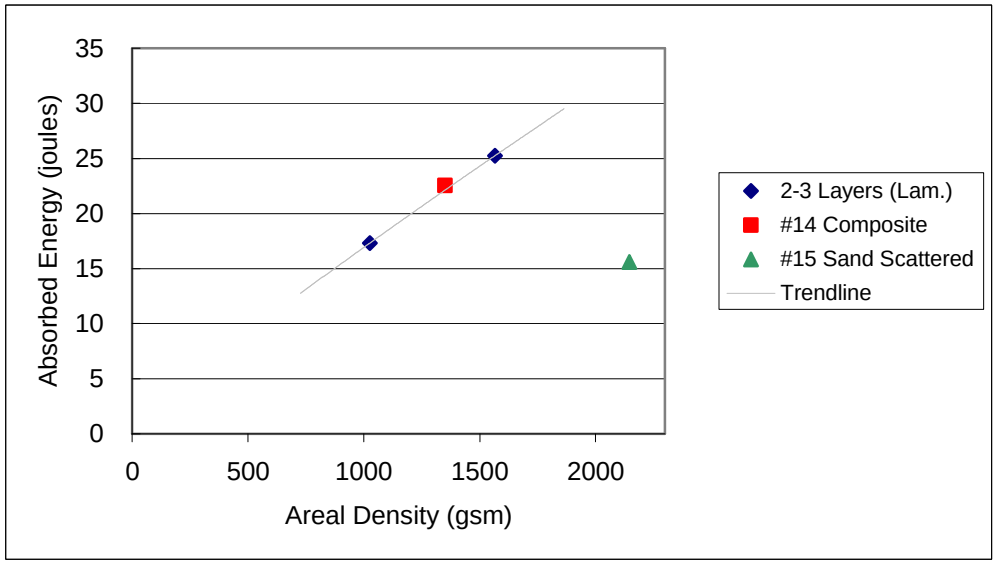

Figure 39. Ballistic Test Results of the Composite and Sand Scattered Structures II (0.22 Magnum Flat Nose)

Sand scattered as a layer structure exhibited significant reduction in total energy absorptions within the ballistic tests of both 0.22 Short HV and 0.22 Magnum Flat Nose bullets. A scattered sand layer decreased ballistic performance about 50%, on a weight basis. This may be explained by the formation of a stiffer structure by the sand particles that are highly exposed to cutting effect.

4.4 Postmortem Inspection

Samples and caught bullets were examined after ballistic tests by using an optical microscope and a camera. Back face, front face and interlaminar failure views were interpreted by the failure region shape and broken yarns of the samples. Also, nose shape deformations of the caught bullets were investigated to interpret ballistic behavior mechanisms.

Pyramid formation on the back face was observed after most of the shooting tests as predicted in literature reviews. Pyramid formations were more distinctive on the targets that absorbed higher energy while not as distinctive in the slide-through effect cases, especially with the sharp nose bullets. But in some of those cases, as shown in Figure 40, pyramid formations were also observed when the bullets did not show slide-through action.

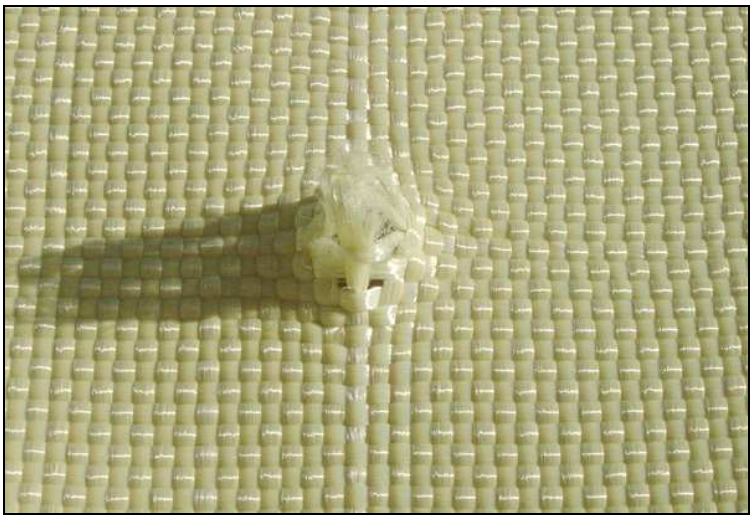

Figure 40. Pyramid Formation on the Back Face of the Target

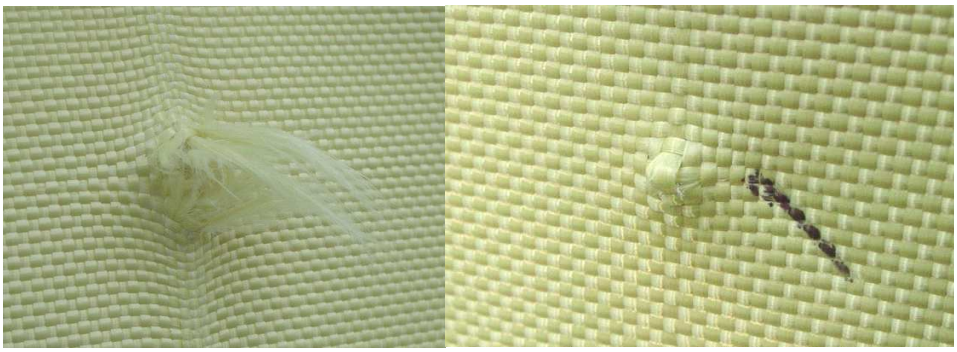

Figure 41. Back Face Deformation of the Targets in the Ballistic Tests with Sharp Nose Magnum Bullets a) 1 BG +1NW b) 2BG + 1NW

Nonwoven layer usage on the outer face increases the friction between the round nose bullets and the primary yarns, and lessens the yarn breakages during the penetration period. After the penetration of the bullet, nonwoven layers showed an additional benefit by increasing the mass of the formed pyramid through traveling with the bullet. The increasing mass provides higher energy absorption and result in some caught bullets, as in Figure 42.

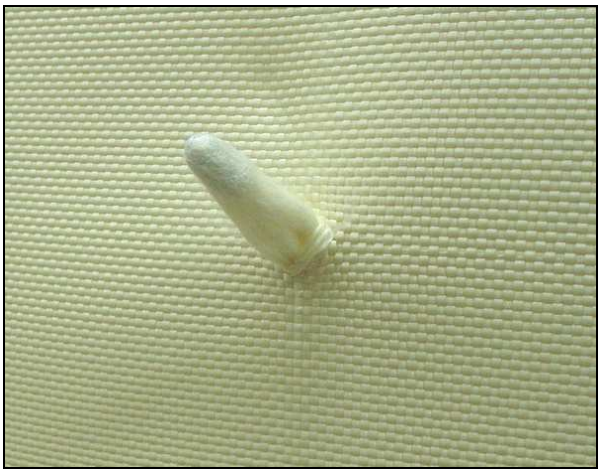

Figure 42. Transit of Nonwoven Layer through the Target I (target: 1BG+1NW, bullet: 0.22 Short)

Figure 43. Transit of Nonwoven Layer through the Target II (target: 1BG+1NW, bullet: 0.22 Short)

Figure 44. Transit of Nonwoven Layer through the Target III (target: 2BG+1NW, bullet: 0.22 Short)

As shown in Figure 45, primary yarns could absorb higher energy and result in bullet caught while their lateral movement action was restricted during the ballistic impact event. This case is a probability of the bullet tip and primary yarn interaction, but the probability could be increased by using a nonwoven facing or laminated structures.

Figure 45. Laterally Restricted Primary Yarns (target: 2BG+1NW, bullet: 0.22 Short)

In some cases, within the tests of laminated structures, bullets changed their route and were reflected back by the targets. As shown in Figure 46, black color on the front face of the target is the contamination that is a result of the friction between yarns and the lead bullet.

Figure 46. Bullet Mark on the Front Face of the Target after Reflection (target: 2BG-Laminated, bullet: 0.22 Short)

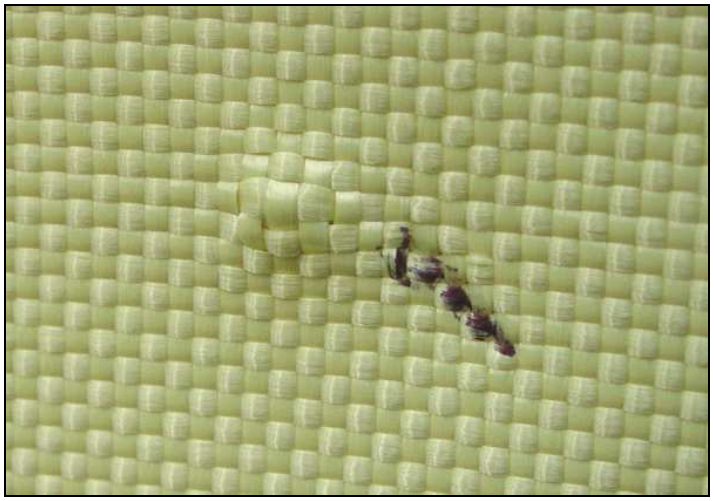

Figure 47. Backface Deformation of the Target through Reflection (Target: 2BG-Laminated, Bullet: 0.22 Short)

As shown in Figure 48, interlaminar delamination actions were observed between the laminated BG fabrics, resulting in some energy absorption.

Figure 48. Delamination between the BG Fabrics in the Impact Zone

Shape deformations of the caught bullets were investigated to clarify the interaction with the yarns. As shown in Figure 49 and 50, side and top views of the caught bullets proved that primary yarns could absorb much higher energy if yarns could not move laterally during the ballistic event.

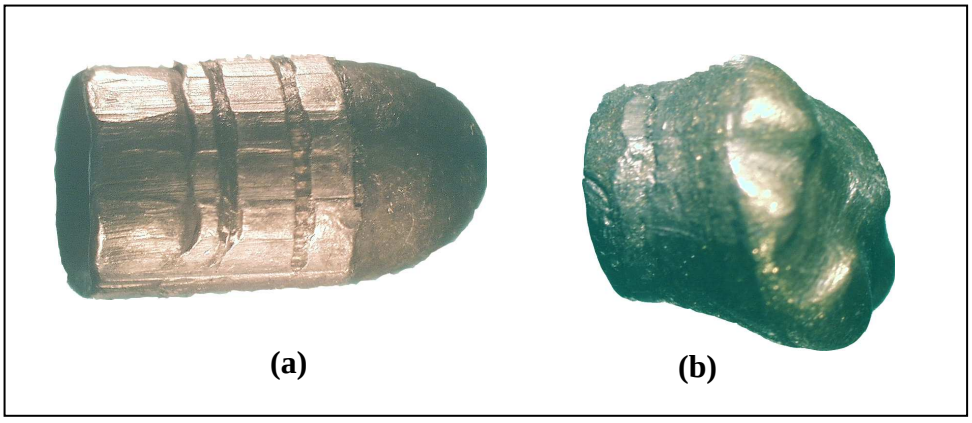

Figure 49. Shape Deformation on the Bullets I (a) original (b) deformed

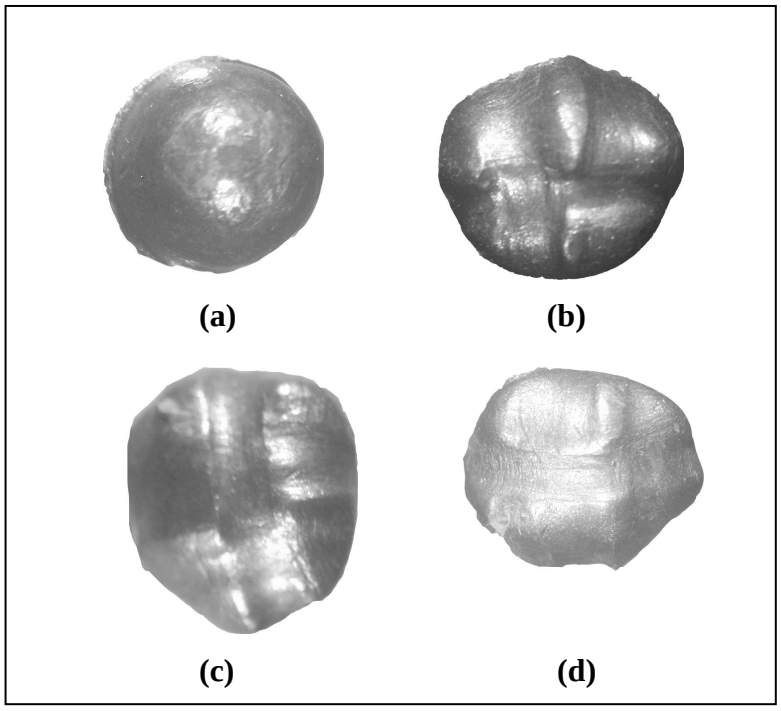

Figure 50. Shape Deformation on the Bullets II (a) original (b,c,d) deformed

CHAPTER FIVE: CONCLUSIONS

The most important conclusions derived from this research are that lamination of the systems with very low resin content (4-6%) are superior to multiple non-laminated systems and this advance could be improved further by hybrid systems using nonwoven fabric layers on the impact side and relatively tighter woven fabrics between the layers. Lamination and relatively tighter woven fabric usage between the layers influence the energy absorbing mechanism indirectly by restricting the lateral movement action of the primary yarns during the ballistic impact event. Although the resin matrix itself did not have much strength, it certainly had an indirect effect on the energy absorption capacity of composites by influencing the number of yarns broken, and perhaps, by a delamination mechanism.

Laminated structures became slightly stiffer, thus, more sensitive to shearing by flat nose bullets. However, the cutting effect was reduced by using a nonwoven facing on the impact side of the systems. On the other hand, the nonwoven facing did not show any improvement when used on the non-laminated systems. In conclusion, nonwoven usage on the impact surface is superior at reducing the cutting effect of the sharp edge nose bullets through the ballistic impact.

Relatively tighter woven fabric, much weaker than ballistic grade fabrics, can increase the energy absorption of the systems by offering possibility to primary yarns of the sequenced fabrics to absorb more energy. They do not break easily when supported

by the adjacent layers and reduce the sliding-through action of the round nose bullets by their relatively tighter structures. Usage of the relatively tighter woven fabric also eliminates the potential slide-through effect provoked by nonwoven facing when used on the impact side of non-laminated systems.

Since, it is difficult to simulate numerically or analytically the ballistic behavior of the hybrid systems because of the complexity of damage mechanism. It is much easier to obtain “before and after” impact data to evaluate the performance of the structures under ballistic impact. Studies of the ballistic impact where the samples fail may allow better analysis of energy absorption while qualification testing provides pass/fail results.

The hybrid systems can offer possibility to construct ballistic protective systems providing higher protection without sacrificing mobility and comfort. It appears that studies are needed to optimize the performance of ballistic textiles through hybrid laminated systems by the layering of different structures.

REFERENCES

[1] http://en.wikipedia.org/wiki/Armour, accessed 11/09/2007

[2] http://www.galls.com/bahistory.html, accessed 11/09/2007

[3] http://en.wikipedia.org/wiki/Body_armor#History, accessed 11/09/2007

[4] http://science.howstuffworks.com/body-armor1.htm, accessed 11/09/2007

[5] http://en.wikipedia.org/wiki/Interceptor_Body_Armor, accessed 11/09/2007

[6] Cheeseman, B.A., and Bogetti, T.A., 2003. 'Ballistic impact into fabric and compliant laminates', *Composite Structures*, 61, pp 161-173.

[7] Duan, Y., Keefe, M., Bogetti, T.A., and Powers, B., 2006. 'Finite element modeling of transverse impact on a ballistic fabric', *International Journal of Mechanical Sciences*, 48, pp 33-43.

[8] Phoenix, S.L., and Porwal, P.K, 2003. 'A new membrane model for the ballistic impact response and V50 performance of multi-ply fibrous systems', *International Journal of Solids and Structures*, 40, pp 6723-6765.

[9] Wardle, M. W., and Tokarsky, E.W, 1983. 'Drop weight impact testing of laminates reinforced with Kevlar aramid fibers, E-glass and graphite', *Comp. Tech. Rev.***,** 5, pp 4-10.

[10] Wardle, M.W., and Zhar, G.E, 1987. 'Instrumented impact testing of aramid reinforced composite materials', *ASTM STP*, 936, pp 219-235.

[11] Thomas, H.L., Ballistic resistant fabric. US Patent 2003/ 0022583, 2003.

[12] Thomas, H.L, 2006. An overview of industrial fabric ballistic protection for police and military personnel. Textile Engineering, Auburn University.

[13] Prosser, R.A., Cohen, S.H., and Segars, R.A., 2000. 'Heat as a factor in the penetration of cloth ballistic panels by 0.22 caliber projectiles', *Textile Research Journal*, 70(8), pp 709-722.

[14] Cunniff, P.M, 1999. 'Decoupled response of textile body', *Proceedings of the 18th International Symposium on Ballistics*, pp 814-821.

[15] Smith, J.C., Blandford, J.M., and Schiefer, H.F., 1960. 'Stress-strain relationships in yarns subjected to rapid impact loading. Part VI: velocities of strain waves resulting from impact', *Textile Research Journal*, 30, pp 752–760.

[16] Roylance, D, 1977. 'Ballistics of transversely impacted fibers', *Textile Research Journal*, 47, pp 679–684.

[17] Morrison, C, 1984. 'The mechanical response of an aramid textile yarn to ballistic impact'. PhD thesis, University of Surrey, UK.

[18] Wilde, A.F., Roylance, D.K., and Rogers, J.M, 1973. 'Photographic investigation of high-speed missile impact upon nylon fabric. Part I: energy absorption and cone radial velocity in fabric', *Textile Research Journal*, 43, pp 753–761.

[19] Briscoe, B.J., and Motamedi, F., 1992. 'The ballistic impact characteristics of aramid fabrics: the influence of interfacial friction', *Wear*, 158, pp 229–247.

[20] Shim, V.P.W., Tan, V.B., and Tay, T.E., 1995. 'Modeling deformation and damage characteristics of woven fabric under small projectile impact', *International Journal of Impact Engineering*, 16, pp 585–605.

[21] Smith, J.C., Blandford, J.M., and Schiefer, H.F., 1960. 'Stress-strain relationships in yarns subjected to rapid impact loading. Part V: Wave propagation in long textile yarns impacted transversely', *Textile Research Journal*, 30, pp 288-302.

[22] Cunniff, P.M., 1992. 'An analysis of the system effects of woven fabrics under ballistic impact', *Textile Research Journal*, 62, pp 495–509.

[23] Roylance, D., and Wang S.S. Penetration mechanics of textile structures. In: Laible RC, editor. *Ballistic Materials and Penetration Mechanics*; Elsevier Publishing Co: New York, 1980.

[24] Field, J.E., and Sun, Q., 1990. 'A high speed photographic study of impact on fibers and woven fabrics'. *Proceedings of the 19th International Congress on High Speed Photography and Photonics Part 2*, pp 703-712.

[25] Cunniff, P.M, 1999. 'Dimensionless parameters for optimization of textile based body armor systems', *Proceedings of the 18th International Symposium on Ballistics*, pp1303-1310.

[26] Chitrangad S. Hybrid ballistic fabric. United States Patent No.5,187,003; 1993.

[27] Tan, V.B.C., Lim, C.T., and Cheong, C.H., 2003. 'Perforation of high-strength fabric by projectiles of different geometry', *International Journal of Impact Engineering*, 28, pp 207-222.

[28] Lee, B.L., Walsh, T.F., Won, S.T., and Patts, H.M., 2001. 'Penetration failure mechanisms of armor-grade fiber composites under impact', *Journal of Composite Materials*, 35, pp1605-1629.

[29] Leech, C.M., Hearle, J.W.S., and Mansell, J., 1979. 'A variational model for the arrest of projectiles by woven cloth and nets', *J. Text. Inst*, 70 pp 469-478.

[30] Gu, B, 2003. 'Analytical modeling for the ballistic perforation of planar plain woven fabric target by projectile', *Composites Part B: Engineering*, 34, pp 361-371.

[31] Naik, N.K., Shrirao, P., and Reddy, B.C.K, 2006. 'Ballistic impact behavior of woven fabric composites: Formulation', *International Journal of Impact Engineering*, 32, pp 1521-1552.

[32] Wu, E., and Chang L., 1995. 'Woven glass/epoxy laminates subject to projectile impact', *Int. J. Impact Eng*., 16, pp 607-619.

[33] Naik, N.K., and Satyanarayana, R.K, 2002. 'Delaminated woven fabric composite plates under transverse quasi static loading: experimental studies', *J. Reinf. Plast. Comp*, 21, pp 869-877.

[34] Freeston, W.D., 1973. 'Strain Wave reflections during ballistic impact of fabric panels', *Textile Research Journal*, 64, pp 348-351.

[35] Dingenan, J.V., and Verlinde, A., 1996. 'Nonwovens and fabrics in ballistic protection', *Tech. Textile Int.*, February, pp 10-13.

[36] Shim, V.P.W., Lim, C.T., and Foo, K.J., 2001. 'Dynamic mechanical properties of fabric armour', *Int. J. Impact Eng.*, 25, pp 1-15.

[37] Ballistic Resistance of Body Armor NIJ Standard 0101.04. National Institute of Justice. http://www.nlectc.org. June 2001

[38] http://www.oehler-research.com/model35.html, accessed 11/09/2007

[39] Cunniff, P.M, 1999. 'The V50 performance of body armor under oblique impact', *Proceedings of the 18th International Symposium on Ballistics*, pp 829-836.

[40] Chitrangad, R., and Parada J.M. Flourinated finishes for aramids. United States Patent No. 5,266,076; 1993.

[41] Chocron, S., Printor, A., Cendon, D., Galvez, F., and Sanchez-Galvez V., 2002. 'Simulation of the ballistic impact in a polyethylene nonwoven felt', *Proceedings of the 20 International symposium Ballistic,* pp 810–816.

[42] Landa, B.P., and Olivares, F.H., 1994. 'An analytical model to predict impact behavior of soft armors', *Int. J. Impact Eng.*, 16, pp 455-466.

[43] Cunniff, P.M., 1999. ‘A semiempirical model for the ballistic impact performance of textile-based personnel armor’, *Textile Research Journal*, 66, pp 45-59.

APPENDICES

Appendix A. Fiber Mechanical Properties [25]

Fiber	Strength (GPa)	Failure Strain (%)	Modulus (GPa)	Density (kg/m^3)	U^* (m/s)
PBO	5.20	3.10	169	1560	813
Spectra® 1000	2.57	3.50	120	970	801
600 denier Kevlar® KM2	3.40	3.55	82.6	1440	682
850 denier Kevlar® KM2	3.34	3.80	73.7	1440	681
840 denier Kevlar® 129	3.24	3.25	99.1	1440	672
1500 denier Kevlar® 29	2.90	3.38	74.4	1440	625
200 denier Kevlar® 29	2.97	2.95	91.1	1440	624
1000 denier Kevlar® 29	2.87	3.25	78.8	1440	621
1140 denier Kevlar® 49	3.04	1.20	120	1440	612

Appendix B. Experimental Setup for Ballistic Test

Appendix C. Cohesive Failure of Laminated Fabrics

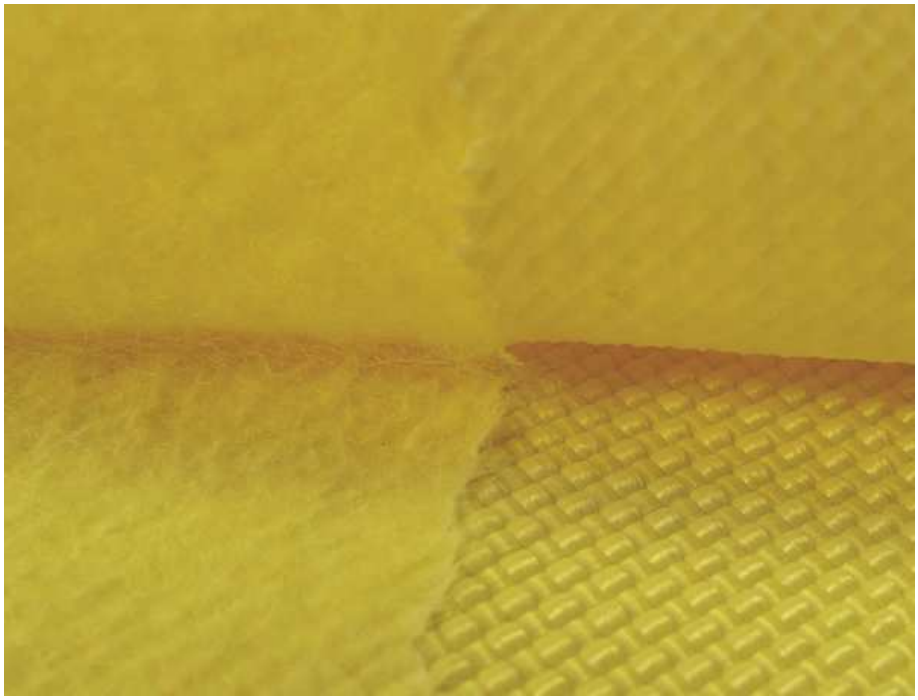

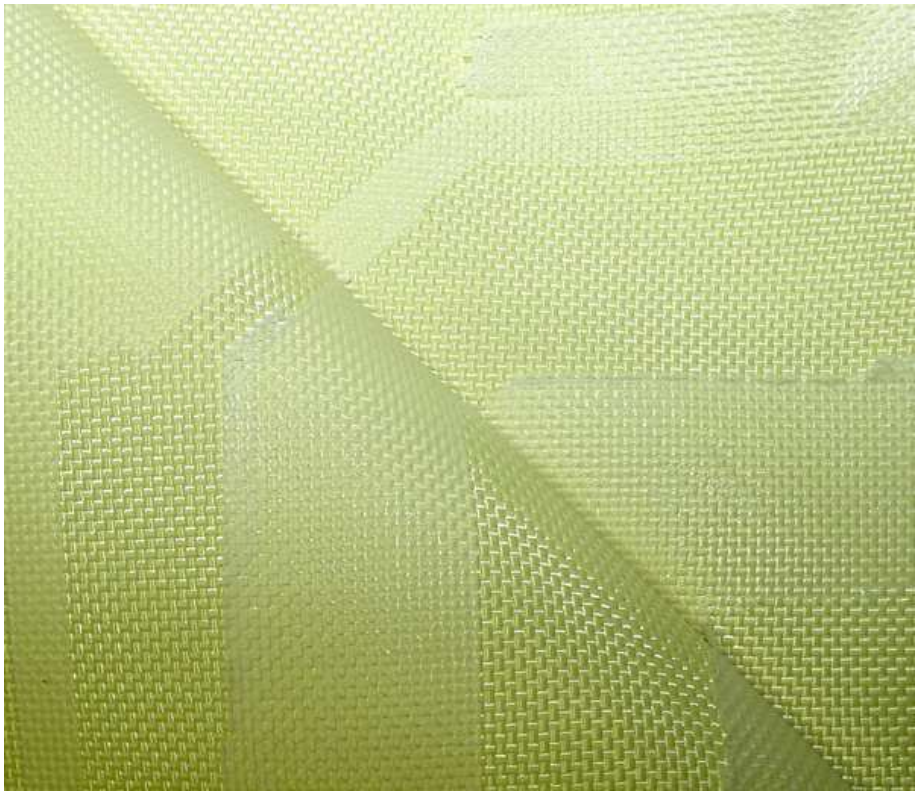

Appendix D. Relative Energy Absorption of Three Different Type of Bullets Through 1, 2 and 3 Layers of BG Fabric

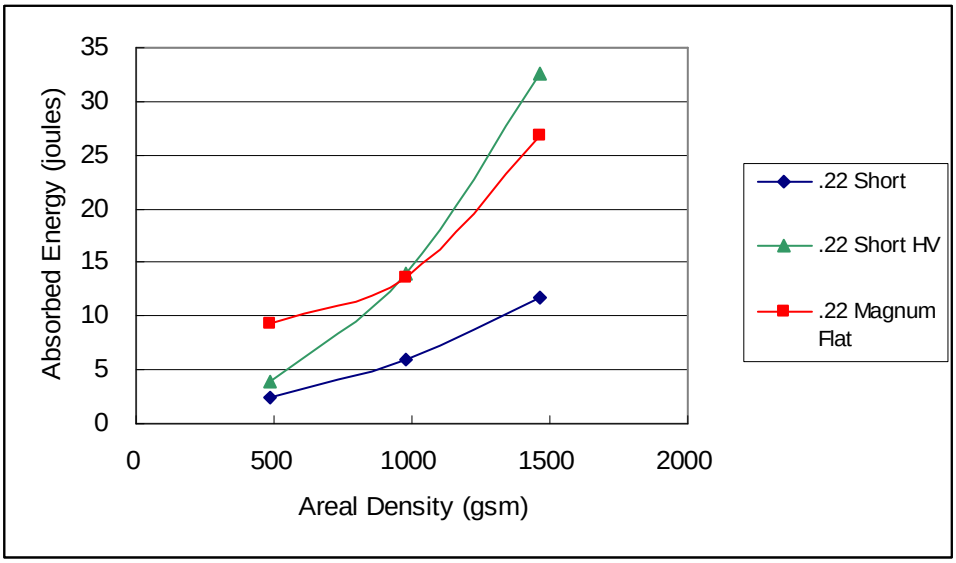

Appendix E. Drop-Weight Impact Test Results of EAA Polymer Film

Sample No	Impact Energy (joule)	Impact Velocity (m/sec)	Energy to Max. Load (joule)	Total Deflection (mm)	Total Absorbed Energy (joule)
1 Layer	46.84	4.21	0.1086	0.91	0.2138
2 Layer	46.57	4.20	0.1681	10.03	0.3771
3 Layer	46.42	4.19	0.4129	12.92	0.6924

Appendix F. Cunniff Ballistic Limit Approach [43]

The model is capable of predicting the performance of the body armor systems according to defined areal density. The model partitions the energy absorbed by the system into strain and kinetic energy, the predominant mechanism of energy absorption is through kinetic energy transfer. System critical velocity (V_c), defined as the highest striking velocity where no penetration occurs, and projectile residual velocity (V_r) can be calculated as follows;

$$V_c = X_8 X_5^{(\sec\theta - 1)} \left(e^{X_6 (A_d A_p / m_p)^{X_7}} + X_9\right)$$

$$V_r = \sqrt{\frac{V_s^2 - V_c^2 e^{-X_3 (V_s - V_c / V_c)^{X_4}}}{1 + X_2 \left(A_d \frac{A_p}{m_p}\right)}}$$

V_s = projectile striking velocity (m/s)

V_c = system critical velocity (m/s)

V_r = projectile residual velocity (m/s)

θ = impact angle (^{o})

A_d = areal density of the system (kg/m^2)

A_p = presented area of the projectile (m^2)

m_p = mass of the projectile (kg)

$X_{2\text{-}9}$ = regression constants

X_2=1.720656409, X_3=0.913045361,

X_4=0.920378651, X_5=1.137412008,

X_6=2.562624057, X_7=0.560704050,

X_8=179.9924122, X_9=0.712318703

Appendix G. Naik-Shrirao-Reddy Ballistic Limit Approach [31]

The method is analytical and based on energy transfer between the projectile and the target. Possible energy absorption mechanisms were described as; cone formation on the backface of the target, deformation of secondary yarns, tensile failure of primary yarns, delamination and friction energy.

$E_{TOTAL} = E_{KEi} + E_{Di} + E_{TFi} + E_{DLi}$

where E_{KEi} = Energy of moving cone, E_{Di} = Deformation of secondary yarns, E_{TFi} = Tensile failure of primary yarns and, E_{DLi} = Delamination energy.

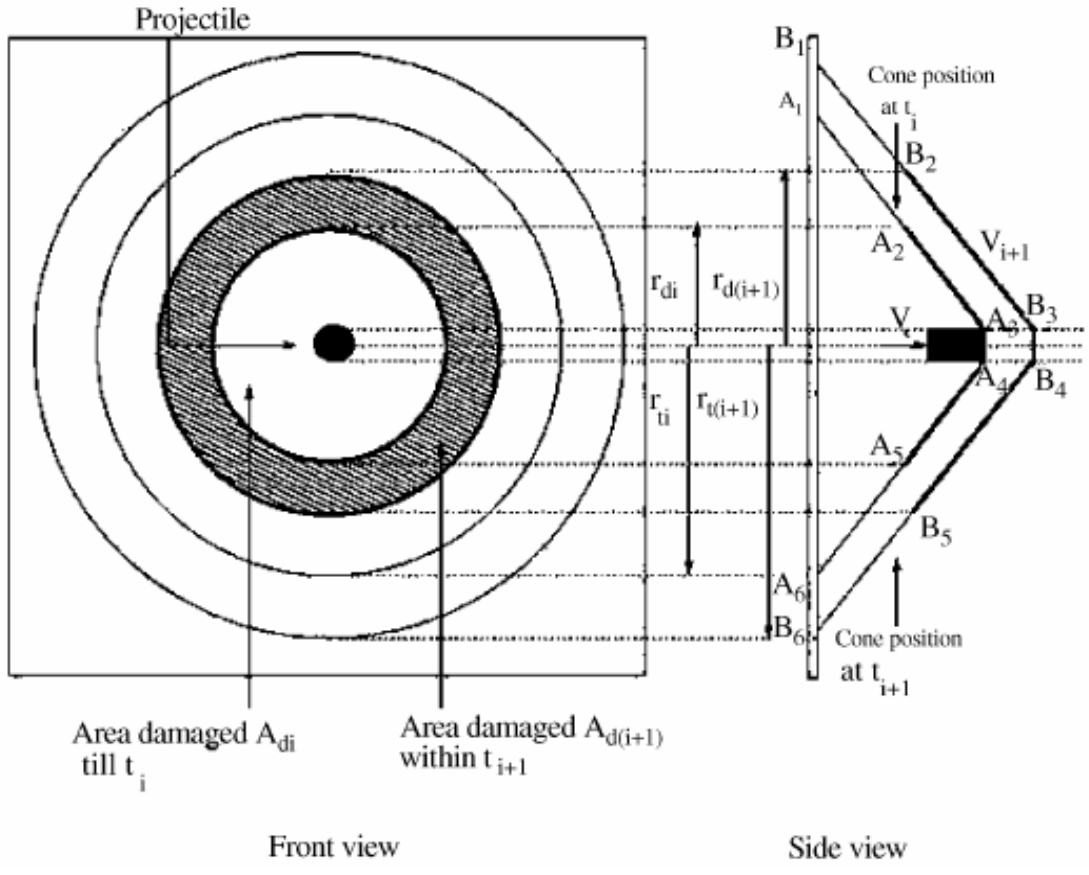

The plastic and the transverse wave velocities are given by,

$$c_p = \sqrt{\frac{1}{\rho}\left(\frac{d\sigma}{d\varepsilon}\right)_{\varepsilon=\varepsilon_p}} \;,\; c_t = \sqrt{\frac{(1+\varepsilon_p)\sigma_p}{\rho} - \int_0^{\varepsilon_p} \sqrt{\frac{1}{\rho}\left(\frac{d\sigma}{d\varepsilon}\right)d\varepsilon}}$$

If the complete impact event is divided into a number of small instants, then at *i*th instant, the time is given by t_i. By that time the transverse wave has traveled to distance r_{ti} and the plastic wave has traveled to a distance of r_{pi}. The projectile has moved through a distance z_i. Radii r_{ti}, r_{pi} and z_i after the time t_i=i Δt is given by,

$$r_{ti} = \sum_{n=0}^{n=i} c_{tn}\,\Delta t \;,\; r_{pi} = \sum_{n=0}^{n=i} c_{pn}\,\Delta t \;,$$

$$\Delta z_i = V_{i-1}\Delta t - \frac{1}{2}\left(\frac{V_{i-1}-V_i}{\Delta t}\right)(\Delta t)^2$$

where;

$$V_i = \sqrt{\frac{1/2(m_p V_0^2 - E_{i-1})}{1/2(m_p + \pi r_{ti}^2 h\rho)}}$$

$$\varepsilon_i = \left\{\frac{(d/2) + \sqrt{(r_{ti} - (d/2))^2 + z_i^2} + (r_{pi} - r_{ti}) - r_{pi}}{b^{(r_{pi}/a)} - 1}\right\} x \left\{\frac{\ln b}{a}\right\}$$

$$\varepsilon_{syi} = \frac{\sqrt{2}(r_{ti} - r)}{(\sqrt{2} r_{ti} - d)}\varepsilon_{pyi}$$

$$E_{KEi} = \frac{1}{2}(\pi r_{ti}^2 h\rho)V_i^2$$

$$E_{Di} = \int_{d/\sqrt{2}}^{r_{ti}} \left(\int_0^{\varepsilon_{syi}} \sigma_{sy}(\varepsilon_{sy})d\varepsilon_{sy} \right) xh\{2\pi r - 8r\sin^{-1}(\frac{d}{2r})\}dr$$

$$E_{TF} = A\int_0^x \left(\int_{\varepsilon=0}^{\varepsilon=\varepsilon_0 b^{x/a}} \sigma(\varepsilon)d\varepsilon \right) dx$$

$$E_{DLi} = \sum_{n=1}^{n=i} \Delta E_{DLn}, \Delta E_{DLi} = P_d \pi(r_{d(i+1)}^2 - r_{di}^2) A_{q1} G_{IIcd}$$

The above process is repeated until all primary yarns in the target fail. The velocity at the end of time interval, during which all the yarns are broken, is the residual velocity of the projectile. On the other hand, if V_i becomes zero, then the projectile does not penetrate the target completely with the given initial velocity.

Nomenclature

a	yarn width	r_{ti}	surface radius of the cone at time t_i
A_{q1}	quasi-lemniscate area reduction factor	t_i	ith instant of time
b	transmission factor	V_i	projectile velocity at time t_i
c_p	plastic wave velocity	z_i	height/depth of the cone at time t_i
c_t	transverse wave velocity	ε	strain
d	projectile diameter	ε_i	maximum tensile strain in primary yarns at time t_i
G_{IIcd}	critical dynamic strain energy release rate in mode II	ε_{sy}	strain in secondary yarns
h	target thickness	σ	stress
m_p	mass of the projectile	σ_{sy}	stress in secondary yarns
P_d	percent delaminating layers	Δt	duration of time interval
r_{pi}	distance covered by plastic wave till time t_i	ρ	density of the target

Appendix H. Landa-Olivares Ballistic Limit Approach [42]

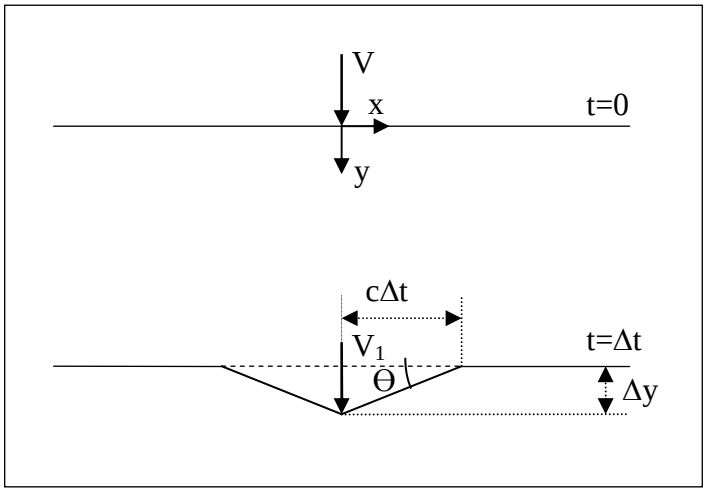

The penetration phenomenon model proposed when the projectile has traveled a distance Δy after Δt seconds. At that moment, the reaction force F decelerating the projectile will be the result of the tension withstood by the yarn in the projectile direction.

$$V_1 = V - a_1 \Delta t \qquad (1)$$

$$F = 2T_1 \sin\theta \qquad (2)$$

$$a_1 = \frac{2T_1}{m}\sin\theta \approx \frac{2T_1}{m}\frac{\Delta y}{c\Delta t} \qquad (3)$$

$$\Delta y = V\Delta t - \frac{1}{2}a_1(\Delta t)^2 \qquad (4)$$

The yarn tensile deformation ε is:

$$\varepsilon = \frac{\sqrt{(c\Delta t)^2 + (\Delta y)^2} - c\Delta t}{c\Delta t} \qquad (5)$$

and the tension withstood by the yarn is:

$$T_1 = SE\frac{1}{2}[(\frac{\Delta y}{c\Delta t})^2 - \frac{1}{4}(\frac{\Delta y}{c\Delta t})^4] \qquad (6)$$

Nomenclature

V	impact velocity of the projectile	T_1	tension force
		m	projectile mass
c	wave speed	S	yarn cross-sectional area

A system of three equations and three unknowns are obtained that are solved by an iterative scheme.

Appendix I. Chemical Structures of the Polymer Films

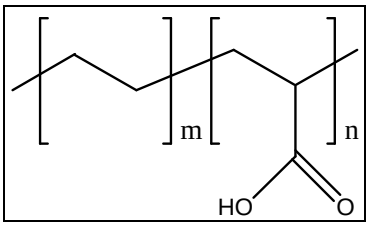

Poly (ethylene-co-acrylic acid)

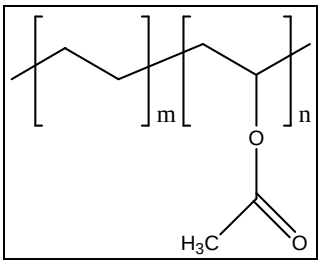

Poly (ethylene-co-vinyl-co-acetate)

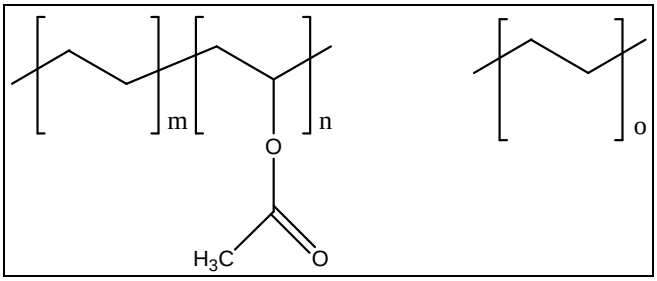

Polymer blend of low density poly (ethylene) and poly (ethylene-co-vinyl-co-acetate)